# ANALYSIS OF EVENT-BASED SOIL HYDROLOGIC RESPONSE FOR DIFFERENT LAND USE TYPES IN UPPER NJORO RIVER CATCHMENT

**LEAH AMISI**

**A thesis submitted to the Graduate School in partial fulfilment for the requirements of Master of Science degree in Agricultural Engineering of Egerton University**

**EGERTON UNIVERSITY**

**NOVEMBER 2018**

## DECLARATION AND RECOMMENDATION

### DECLARATION

This thesis is my original work and has not been presented before in any other institution known to me for award of a Degree or any other award.

Signature…… Date ……

**Leah Amisi**
BM11/ 14482/15

### RECOMMENDATION

This thesis has been submitted for examination with our recommendation and approval as University supervisors.

Signature…… Date ……

**Dr. Peter M. Kundu**
Department of Agricultural Engineering
Egerton University

Signature…… Date ……

**Dr. Raphael M. Wambua**
Department of Agricultural Engineering
Egerton University

## COPYRIGHT

## ACKNOWLEDGEMENT

My sincere gratitude goes to the Almighty God for His divine assistance and the grace that has sustained me this far. To God be the glory. Thanks to the Egerton University for giving a chance to study and access learning resources within the Department of Agricultural Engineering.

Gratitude to my supervisors Dr. Peter M. Kundu and Dr. Raphael M. Wambua for the regular discussions, suggestions and continued guidance which has contributed to the completion of this work. I also thank the staff in the Faculty of engineering for their support.

My heartfelt gratitude also goes to the African Development Bank in collaboration with the Ministry of Higher Education and Technology for the scholarship. I acknowledge Dr. Vincent Odongo for reading and positively critiquing my work. I recognize the support from the research assistants Mr. F. Okinda and Mr. E. Amisi during field work. Last but not least, I thank my dad Mr. Joseph Ng'anga, spouse Stephen Musindayi and daughter Bethangel Musindayi for the patience, continuous love and support during the study period.

## DEDICATION

To the Almighty God, to my loving dad Joseph Ng'anga and Uncle James Makali for encouraging me to pursue education to high levels. I also dedicate this work to my caring husband Stephen Musindayi and daughter Bethangel.

## ABSTRACT

Land use/cover change alters the hydrologic response of river catchments. The response depends on the soil characteristics such as; infiltration capacity, porosity, organic matter content and bulk density. Understanding the effect of the land use change on soil hydrologic response in Upper Njoro River catchment is crucial for formulation and adoption of proper soil and water conservation techniques for increased agricultural production. Additionally, the characteristics of extreme events in terms of magnitude, frequency and duration are key to proper planning and management of water resources. The objective of this research was to evaluate event-based hydrologic soil hydrologic response for different land use types in Upper Njoro River Catchment. Randomized Block experimental design was used where four land use types were purposely selected and blocked against soil hydrologic response parameters and soil properties. The land use types included; natural forest, deforested land, fallow agricultural land and grassland having been indicated to be the major land use types within the catchment. The evaluated soil hydrological response parameters included runoff coefficients, infiltration rate, and water repellency and ponding time and soil properties. Gross rainfall partitioning across planted trees and characterization of annual peak discharges for Njoro River using selected probability distribution functions was also carried out. The findings showed fallow agricultural land, grassland and natural forest to have textural classes of sandy clay loam, clay loam and loam respectively based on USDA textural triangle. The highest and lowest mean bulk densities of 1.36 and 0.96 g/cm$^3$ were found in deforested and natural forest land respectively. The highest mean saturated hydraulic conductivity of 170.21 cm/day, porosity of 0.62 and organic matter content of 4.63% were observed in the natural forest while the lowest values of 24.78 cm/day, 0.47 and 0.75% respectively were found in the deforested land. High water repellency of 18 seconds penetration time and runoff coefficient of 0.0077 were observed in the deforested areas. The quantified rainfall partitions was 43.04% for stem and through flow and 56.96% for interception. The best fitting probability distribution model was found to be Generalized Pareto. Peak flow discharges estimated for 50, 100 and 200 year return periods using the best fitting model included 8.1 m$^3$/s, 10.1 m$^3$/s and 12.3 m$^3$/s respectively. The results showed that deforestation has affected soil hydrologic response and soil properties negatively. The study provided understanding of on-site effect of different land use types on hydrological functioning of soils which in turn affect response of stream flow. Future work should aim at restoring the hydrological functioning of soils within the catchment.

## TABLE OF CONTENTS

## LIST OF TABLES

## LIST OF FIGURES

## LIST OF ABBREVIATIONS AND ACRONYMS

| Acronym | Description |
|---|---|
| ANOVA | Analysis of Variance |
| AWHC | Available Water Holding Capacity |
| CN | Curve Number |
| DBH | Diameter at Breast Height |
| DPC | Dump Proof Course |
| I | Interception |
| FC | Field Capacity |
| GIS | Geographical Information System |
| GR | Gross Rainfall |
| LCLUC | Land Cover and Land Use Change |
| K | Potassium |
| MFC | Mau Forest Complex |
| PRMS | Precipitation Runoff Modeling System |
| PWP | Permanent Wilting Point |
| SCS | Soil Conservation Service |
| SF | Stem Flow |
| SWAP | Soil Water Atmosphere and Plant |
| SWAT | Soil and Water Assessment Tool |
| SWMM | Storm Water Management Model |
| TF | Through Flow |
| USA | United States of America |
| UNRiC | Upper Njoro River Catchment |
| USDA | United States Department of Agriculture |
| USGS | United States Geological Survey |
| SOC | Soil Organic Carbon |
| WDPT | Water Drop Penetration Test. |

## DEFINATION OF TERMS

| Term | Definition |
|---|---|
| **Land use/land cover change (LULCC)** | Human modification of Earth's terrestrial surface or may refers to all processes leading to land cover and land use changes for instance deforestation, expanse of agricultural land, urbanization, drainage of wetlands |
| **Land use** | Human uses of the land, including actions that modify or convert land cover from one type to another. |
| **Land cover** | Physical characteristic of the earth's surface captured in the distribution of vegetation, water, desert, ice, and other physical features of the land including those created solely by human activities such as settlement. |
| **Deforested land** | An area that where trees have been cut and the land has been left bare. |
| **Soil hydrologic response** | How quick an effect is realized on soils as a rainfall storm begins. |
| **Event-based hydrological analysis** | Monitoring how a catchment responds to an individual rain fall event |

## LIST OF APPENDICES

# CHAPTER ONE
# INTRODUCTION

## 1.1 Background Information

Land use types have been reported to influence hydrologic response in river catchments. According to Guzha *et al.* (2018), forest cover loss leads to increased stream discharges and runoff volumes. Deforestation in the tropical forests has been the focus of scientific and political discussion in the recent past. This is because deforestation has led to surface energy fluxes and dynamics in hydrological and carbon cycles (Dos Santos *et al*., 2018). Guzha *et al.* (2018) carried out a study on the impact of different land use types on surface runoff, discharge and low flows and showed that forest cover loss in the catchment is accompanied by increased stream discharges and surface runoff. Forest land contributes more to water yield due to increased infiltration as compared to built up areas and other land use types which have reduced infiltration rates (Lu *et al*., 2015).

Studying the changes in soil properties caused by different land uses allow measures to be adopted to reduce the risk of future negative effects (dos Santos *et al*., 2018). Changes in infiltration capacity and soil water repellency are good parameters and indicators of soil hydrological functioning of a given catchment. Patil *et al*. (2018) observed that soil infiltration capacity is key parameter influencing the occurrence of soil hydrologic response. Assessment of the impacts due to land use types on soil hydrologic response at regional scale is difficult due to limited information on soil properties and land use types (Abu-Hashim *et al*., 2011). Infiltration capacity is controlled by soil hydraulic properties and can effectively be determined by field and laboratory measurement (Toffour *et al*., 2018). Benavides *et al*. (2018) noted that the capacity to regulate water flow into the soils depends on specific soil characteristics such as infiltration rate, porosity, organic matter content and bulk density. Alteration of the soil physical properties that control infiltration and transmission of water and construction of roads that re-route water to different directions causes changes in soil hydrologic response.

Upper Njoro River catchment (UNRiC) falls within the Eastern Mau forest situated along the western escarpment of the Rift Valley. It serves as the head water for Njoro River which is the major river draining its water in Lake Nakuru. Over the past years, Upper Njoro River catchment (UNRiC) has undergone significant land use changes due to increased human population demanding land for settlement and subsistence agriculture (Ouko *et al*., 2016). The

impact of human activities has gradually increased forcing the government to resettle people living in the forest. Changes in the catchment hydrology have been noted in (URiNC) where River Njoro appeared to become seasonal and boreholes were drying up (Mwetu, 2010). Previous researchers such as Kundu *et al*. (2004) and Baker & Miller (2013) used annual data available in the weather and hydro metrological stations to analyze the effect of land use change on hydrology using hydrological models. Their findings showed that URiNC had undergone dynamic land use change leading to changes in hydrologic regimes. Variations in the stream flows, increased runoff and reduction in infiltration have also been reported (Baker & Miller, 2013). There being some efforts of reforestation within the catchment, there is hope for the reduction of overland flow. It was shown by Owens *et al.* (2006) that partitioning of gross rainfall into canopy interception, litter interception, stem flow and through fall allows estimation of physical impact of trees on local hydrologic budget. There also exist hydraulic structures such as dams which receive water mainly from runoff. Frequency analysis of flows and there durations is important in selection of the best probability distribution model which can be used in estimating flows for design of dams, culverts bridges and other hydraulic structures ( Afreen & Muhammad, 2012; Ahmad *et al*., 2015; Lee *et al*., 2017).

In this study, characterization and quantification of hydrological response parameters in different land use types at plot scale was conducted. The key soil hydrologic response parameters that were determined included: water repellency, ponding time, runoff coefficients and infiltration rate. Rainfall partitioning of planted trees was also carried out to determine their effectiveness in rainfall interception. It was also imperative to select the best probability distribution function for analysis of peak flows to provide information that can be used in for the design of dams design and other hydraulic structures within the UNRiC. This allows proper measures to be taken to reduce future negative effects as a result of deforestation.

### 1.2 Statement of the Problem

Upper Njoro River Catchment (UNRiC) has undergone significant deforestation due to human activities. Increased run-off rates and decreased infiltration rates have been reported. Additionally, soil properties that influence hydrologic response such as; saturated hydraulic conductivity and bulk density have deteriorated. In this research, on-site event-based and land use types are correlated to the soil hydrological response parameters which is not clearly investigated by previous researchers within the catchment. There being efforts of reforestation

in the catchment, there is limited knowledge on rainfall partitioning by planted trees. Seasonal variation of flows in Njoro River have been reported and there exist hydraulic structures such as dam within the catchment. However, there is inadequate research on best fitting probability distribution function that can be used in frequency analysis of peak discharges which is crucial in design of dams and other hydraulic structures. Due to inadequate continuous monitoring of hydrological data within the catchment there was need for event-based monitoring.

### 1.3 Objectives

The broad objective of the study was to evaluate the event-based soil hydrologic response from different land use types in the Upper Njoro River Catchment.

The specific objectives were to;

i. Determine the effect of different land use types on event-based soil hydrologic response and soil properties within the Upper Njoro River catchment
ii. Determine the event-based gross rainfall partitions for planted trees within Upper Njoro River catchment
iii. Compare the performance of different probability distribution functions on estimating peak discharges for different return periods in Upper Njoro River Catchment

### 1.4 Research Questions

i. How do different land use types affect the soil hydrologic response and soil properties in Upper Njoro River Catchment?
ii. How do event-based rainfall partitions compare for management of water resources within Upper Njoro River Catchment?
iii. How do different probability distribution models compare in analyzing of peak flows and recurrence in Upper Njoro River Catchment?

### 1.5 Justification

The study was necessary in providing information to water resource managers to minimize undesirable impacts of deforestation on streamflow. Knowledge on the trends in soil hydrologic processes was needed to provide baseline data for future soil and water relations research.
Information on rainfall partitioning of the tree species within the catchment was important in balancing afforestation and water resource manager's needs. Knowledge on extreme flow analysis and return period was necessary for planning, design of hydraulic structures and risk

management within the catchment. The study also helps in the realization of sustainable development goal 15 which entails combating desertification, restoration of degraded land and soil. Knowledge on extreme flow analysis and return period is essential for planning, design of hydraulic structures and risk management.

### 1.6 Scope and Limitations

The field work was carried out in Upper Njoro River catchment for four months from September to December, 2017. The research employed experimental approach where soil hydrologic response parameters and the associated soil properties were determined in four land use types. Rainfall partitioning of planted trees within the catchment was also carried out. However the study was limited to near soil surface hydrologic parameters and only one species of trees was used for rainfall partitioning. The experiment was also limited to four land use types that included natural forest, fallow agricultural land, grassland and deforested land. The stream flow data used for frequency analysis was from one gauging station which had consistent and adequate data availability.

# CHAPTER TWO
# LITERATURE REVIEW

## 2.1 Soil Hydrologic Response

Soil hydrologic response refers to how quick an effect is realized on soils as a rainfall storm begins. Hydrologic response refers to how fast a stream flow increases at the beginning of rainfall or snowmelt (Winkler *et al*., 2010). Hydrological response depends on the form of precipitation, antecedent precipitation index (API), catchment characteristics and the flow paths along which water is delivered through the catchment to the stream channel Winkler (*et al*., 2010). The flow paths can change as a result of soil compaction during deforestation. As indicated by Havel *et al*. (2018) wild fires causes changes in hydrologic response. Tillage and overgrazing affects soil properties and damages soil hydrological properties (Gol & Yilmaz, 2017). Benavides *et al*. (2018) observed that different land use types that involved agricultural activities and grazing posed a threat on the soil properties hence reducing their efficiency in storing and regulating water flow.

According to Winkler *et al*. (2010), clearing of forests has a significant effect on sub-surface hydrologic response as it leads to decreased interception and evaporation of water. The changes in infiltration capacity in changes the pathways that water takes towards the stream and therefore stream flow response to rainfall and water quality changes (Buttle *et al*., 2018). The groundwater resources are decreasing over time as less amount of rainfall is contributing to natural recharge on one hand there is rapid infrastructure development (Chandramouli & Natarajan, 2016). Event-based monitoring of data sets provides similar information for soil hydrologic response as continuous monitoring during rainy season (Correa *et al*., 2016). There was limited research on the effect of different land use types on soil hydrologic response within Upper Njoro River Catchment .The main factors that may lead to physical changes in the soil hydrologic processes include; loss of duff and O-horizon, soil sealing and soil hydrophobicity.

### 2.1.1 Duff and O-Horizon

Duff and O horizon are the most distinctive features of forest ecosystem and mainly consists of vegetation parts such as leaves, branches, bark and stems existing in various stages of decomposition. Forest soils tend to have greater infiltration rates because of the high percentage of macro pores generated by old root channels, and/or burrows and tunnels made by animals, insects and worms and have the ability to exceed rainfall rates of 12 cm per hour (Ice *et al*.,

2004). Fisher & Binkley (2000) observed that mature forests have thick O horizons underlain by deep soils, both of which rapidly absorb water like a sponge and result to delayed hydrologic response. Undisturbed, mature forest soils generally have little surface runoff and the thick O-horizon protects the soil surface from rain drops impact thus lessening soil particle detachment and overall erosion during storms. Therefore forest clearing reduces the duff and O horizon hence lowering the soil water storage of the catchment. Additionally, clearing of forests through burning leads to fire-induced soil water repellency. The formation of hydrophobic layer restricts water movement downward through the soil profile, thereby reducing the water holding capacity of the soil. A reduction in water holding capacity contributes to saturation excess overland flow (Ice *et al.*, 2004). Destruction of the duff and O-horizon also exposes bare soil to rainfall impact that can lead to erosion through particle detachment (Onda *et al.*, 2008).

### 2.1.2 Soil Sealing

Soil sealing can contribute to significant increases in excess overland flow. Reduced surface cover subjects bare ground to processes that cause soil sealing. Two types of seals that can form include; structural and depositional. Structural seals develop as a result of soil compaction, slaking, pore clogging, and destruction of soil aggregates by direct rainfall impact. Depositional seals form by the settling of fine particles carried in runoff (Assouline & Mualem, 2000). The inability of water to infiltrate the upper soil layers leads to increase in excess overland flow.

Zwartendijk *et al.* (2017) carried out a study on the effect of forest regrowth on infiltration capacity and flow pathways in Eastern Madagascar using experimental approach. The findings showed that infiltration in mature forests was characterized by macro-pores flow while exhausted agricultural land was characterized by matrix flow. Similar findings were obtained by Lin & Zhou (2008) observed subsurface preferential flow on concave hill slopes, convex hill slopes and valley floor in Shale Hills catchment. The results led to a conclusion that combined consideration of soil types and landscape features were important to ensure proper use of soil data for hydrological application. In Njoro River catchment, Mwetu (2010) modelled the responses of hydrology to land use change and climate variability using SWAT model and found that land use change had led to reduced infiltration rates and increased surface runoff.

## 2.2 Effect of Different Land Use Types on Soil Properties

The physical properties of soil influence farm operations and the level of micro-biological activities of a given soil, water and air that is available to plants. Generally, change in land cover and land use affect most physical properties of soil. A study by Haghighi *et al.* 2010 showed that total porosity, mean-weight diameter of aggregates, saturated hydraulic conductivity, available water content and final infiltration rate varied significantly for different land use types. Soil properties influence infiltration rates and the main driving forces are hydraulic conductivity and water holding capacity. The soil properties that have association to infiltration rates are soil texture, structure, composition, and degree of compaction, which influence soil matrix forces and pore space. In addition, antecedent water content, type of vegetative or other ground cover, slope, rainfall intensity and movement and entrapment of soil air are important factors that also affect infiltration rates. Moges *et al.* (2013) carried out a study on land use effects on soil quality indicators in Ethiopia and found bulk density, soil organic carbon (SOC) and available potassium (K) to vary significantly with land use and soil depth. The conclusion from the study showed that soil quality can be protected and maintained by improving existing land use practices within agricultural and forest lands.

As indicated by Mwetu (2010), Upper Njoro River Catchment is characterized by Mollic Andosols which are mainly volcanic ash but contain small quantities of tuff, pumice, cinders and other volcanic ejects. Soil aggregate stability and hydraulic conductivity are highest in forest land and decreases in the order of grassland, agriculture and wetland respectively. A study by Okelo *et al.* (2015) in five land use types of Njoro River catchment that included agriculture, grazing, indigenous forest, deforested and plantation indicated that organic matter ranged from 5.0 to 10.1 % and was highest in the deforested area. Bulk density ranged between 0.74 to 1.05 g/cm$^3$ with grazing land being the highest. Soil water content, soil pH and soil texture ranged from 22.4 and 29.2 and 5.8 to 6.4 for clay loam-sandy and clay loam respectively.

In relation to volume of soil, the soil water content is given by;

$$\theta = \frac{V_W}{V_T} \tag{2.1}$$

where; θ = Volumetric water content (ratio)

$V_W$ = the volume of water (cm$^3$)

$V_T$ = the bulk volume of soil ($cm^3$)

In relation to mass of dry soil, water content is expressed as;

$$\omega = \frac{m_w}{m_s} \tag{2.2}$$

where; ω = gravimetric water content (ratio)

$m_w$ = the mass of water (g)

$m_s$ = the mass of dry soil (g)

The hydraulic conductivity of the soil is critical to infiltration rate since it expresses how easily water flows through soil and is a measure of the soil's resistance to flow. A study by Mainuri & Owino (2013) in Upper Njoro River Catchment showed that there was a negative correlation between hydraulic conductivity, bulk density and clay content

Based on Utin & Oguike (2018) who applied Darcy's law to determine the saturated hydraulic conductivity after an outflow rate, Darcy equation is given as shown.

$$K = \frac{QL}{hA} \tag{2.3}$$

where;

$K$ = hydraulic conductivity (cm/s)

$L$= Length of sample (cm)

$A$ = Cross-section area of sample ($cm^2$)

$h$ = fluid head difference (cm)

Bulk density is the ratio of soil to volume of dry soil. It is used as a measure of soil wetness, volumetric water content and porosity. It influences compactness which is a measure of soil structure, for calculating soil pore space and as indicator of aeration status and water content. Bulk density also provides information on the environment available to soil micro-organisms. The study results of Bewket & Stroosnijder (2003) and Lemenih (2004) showed that the bulk density of cultivated soils was higher than the bulk density of forest soils. Bulk density increased in the 0-10 and 10-20 cm layers relative to the length of time the soils were subjected to cultivation (Lemenih, 2004). The changes in the physical soil attributes on the farm fields can be attributed to the impacts of frequent tillage and the decline in Soil Organic Matter (SOM)

content of the soil (Negassa, 2001). Bulk density is given by equation 2.3 based on Utin & Oguike (2018) who applied the equation.

$$\rho_T = \frac{m_S}{V_T} \tag{2.4}$$

where: $\rho_T$ = bulk density (g/cm$^3$)

$m_s$ = the mass of dry soil (g)

$V_T$ = the bulk volume of soil (cm$^{3)}$

There was need to examine how different soil properties are affected by different land use types since soil hydrologic response depends on the soil characteristics such as infiltration capacity, porosity, organic matter content and bulk density (Benavides *et al*., 2018).

**2.3 Runoff**

The process of runoff can be defined as the residue of precipitation after evaporation and infiltration which propagates into stream channels, lakes and oceans as surface, subsurface and base flow. The nature of runoff in a given catchment indicates whether the catchment has been affected by land cover and land use change. A study conducted by Croke *et al.* (2004) showed that land use change is an important factor in the runoff process that affects infiltration, erosion and evapotranspiration. Rapid land use changes results to decrease in the soil permeability, and consequently increase the amount and rate of runoff. The runoff rate changes in amount of water that flows out of the catchment area, timing and regulation of flow and quality of water. Runoff and ground water are mainly lateral flows and connect each plot to its landscape context. The amount of runoff is controlled by factors like rainfall duration and intensity, vegetation cover, soil moisture content, meteorological conditions before the storm, land slope and soil type. Storms of longer duration but less intensity can result in runoff since infiltration rates tend to decrease with time as rainfall duration. The runoff generation mechanism can be either saturated overland flow or infiltration excess runoff flow.

Some of the specific models that have been developed for describing runoff include; Soil conservation service (SCS) curve number (CN) model, Storm water management model (SWMM), Hydrus 1D and Soil water atmosphere and plant (SWAP) model. The models are discussed in details under the following;

### 2.3.1 Storm Water Management Model (SWMM)

Storm Water Management Model (SWMM) is a dynamic rain-runoff simulation model used for single event or long-term simulation of runoff quantity and quality from urban areas (Niazi *et al*., 2011). The author also noted that SWMM conceptualizes a sub-catchment as a rectangular surface that has a uniform slopes S and width W that drains to a single outlet of the channel hence Manning's equation can be used to express runoff as shown.

$$Q=\left(\frac{1.49}{n}\right)\times S^{\frac{1}{2}}\times R_x^{\frac{2}{3}}A_x \qquad (2.5)$$

where;

$Q$ = Surface runoff ($m^3/s$)

$n$ = Surface roughness coefficient

$S$ = Apparent or average slope (m/m)

$A_x$ = Area across the sub-catchment width through which the runoff flows ($m^2$)

$R_x$ = Hydraulic radius associated to area (m).

SWMM does not consider the detailed physical processes directly yet hydrologic performance of vegetation under precipitation event is required to obtain results of hydrologic response. It has limited ability to simulate measured runoff in vegetated areas.

### 2.3.2 Soil Water Atmosphere and Plant (SWAP)

The model is widely used and was designed to simulate flow and transport processes at site scale for long term time series. SWAP model applies Richard's equation integrally for the unsaturated-saturated zone using possible transient and perched ground water levels (Kroes *et al*., 2009). Based on Kroes *et al*. (2009) who indicted the governing equation for water flow to be as shown.

$$\frac{\partial\theta}{\partial t}=\partial\left(K(h)\left(\frac{\partial h}{\partial z}+1\right)\right)-S_a(h)-S_d(h)-S_m(h) \qquad (2.6)$$

where;

$\theta$ = Volumetric water content ($cm^3/cm^3$)

$t$ = Time (days)

$S_a(h)$ = Soil water extraction rate by plant roots ($cm^3/cm^3/d$)

$S_d(h)$ = Extraction rate by drain discharge in the saturated zone (per day)

$S_m$ *(h)* = Exchange rate with macro-pores (per day)

$K$ = Hydraulic conductivity (cm/day)

$h$ = Soil water pressure head (cm)

$z$ = Vertical coordinate (cm)

It simulates the physical movement of water, atmospheric boundary conditions and plant water uptake but it is limited in simulation of runoff therefore not suitable for this study.

### 2.3.3 HYDRUS Model

As indicated Hilten et al. (2008) HYDRUS model numerically solves the Richard's equation for saturated-unsaturated water flow and convection, dispersion equation for heat and solute transport. The HYDRUS model is governed by the following equation;

$$\frac{d\theta}{dt} = \frac{d}{dx}\left[K(h)\frac{dh}{dx}\right] + \frac{d}{dy}\left[K(h)\frac{dh}{dy}\right] + \frac{d}{dz}\left[K(h)\frac{dh}{dz} + \right] - S_w \tag{2.7}$$

where;

$\Theta$ = the volumetric water content ($m^3/m^3$)

$t$ = time (hours),

$h$ = the soil water matrix head (m)

$x, y, z$ = spatial coordinates (m)

$S_W$ = sink term which represents the volume of water removed per unit time from a unit volume of soil ($m^3/s$)

$K$ *(h)* = the saturated hydraulic conductivity (m/day)

However, the model was not applicable in the study since the work was evaluating sub- surface soil hydrologic response parameters.

### 2.3.4 Soil Service (SCS) Curve Number (CN) Model

The Soil Conservation Service (SCS) curve number (CN) method is among the methods that have been used to estimate runoff. It was developed by USDA in 1954 based on water balance equation and two fundamental hypotheses. The first hypothesis is that the ratio of actual amount of direct runoff to maximum potential runoff is equal to the ratio of the amount of actual infiltration to the amount of potential maximum retention (Mishra & Singh, 2013).

$$Q = \frac{(P - I_a)^2}{(P - I_a + S)} \tag{2.8}$$

where;

$Q$ = runoff (mm)

$P$ = rainfall (mm).

$I_a$ = initial abstraction (mm)

$S$ = potential maximum retention after the runoff begins (mm)

Expressing the equation 2.5 mathematically by replacing the function below in the equations;

$$P_e = P - I_a \tag{2.9}$$

$$S_e = S - I_a \tag{2.10}$$

The runoff function therefore becomes:

$$Q = \frac{P_e^{\,2}}{P_e + S_e} \tag{2.11}$$

where;

$S_e$ = depth of effective available storage (mm)

$P_e$ = effective precipitation (mm)

Effective available storage, $S_e$, depends on the moisture status of the catchment and can vary from some maximum $S_{e(max)}$ when the catchment is dry to minimum $Se_{(min)}$ when the catchment is wet (Schneiderman *et al.*, 2007). This parameter can be calibrated with the measured runoff in the watershed whether it represents the saturation excess runoff in the watershed or not. While calibrating the effective available storage, the effective rainfall can also be calculated by subtracting reference evapotranspiration ($ET_O$) from rainfall (Engda *et al.*, 2011). The main advantages of the model as indicated by Mishra & Singh (2013) include; it is easy to understand and apply, stable and useful for ungauged watersheds. It is also able to account for most runoff producing watershed characteristics like soil type, land use, surface conditions and antecedent moisture conditions. However as noted by Mockus (1964), it does not contain an expression for time and ignores the impact of rainfall intensity and its temporal distribution hence not used in this study. Direct measurement of runoff was done in runoff plots for this study.

## 2.4 Infiltration and Ponding Time

Infiltration refers to the entry of water into the soil through its soil-air interface. The rate at which infiltration occurs is termed as infiltration rate. As indicated by Rawls (1993), movement of water in the soil continues even after infiltration to enhance ground water recharge. Skaggs & Khaleel (1982) reported that the knowledge of factors affecting infiltration rates is not only important for determination of surface runoff, but also helps in understanding subsurface movement and storage of water within a catchment. Infiltration rate is influenced by soil properties and slope on a large extent. Slope has a dominant effect on the contribution of rainfall to stream flow and to the groundwater reservoir in as much as it controls the duration of overland flow, infiltration and subsurface flow. A flat ground surface allows more infiltration to occur than a steep ground surface that encourages more surface runoff into streams. The slope conditions also control the depth to the water table and distribution of head and artesian pressures in aquifers. Rainfall intensity also determines the infiltration rate and is obtained by dividing the depth of rainfall by the duration of rainfall for a uniform storm or rainfall. Ponding time is that period when infiltration rate equals to precipitation rate.

A study by Kutílek & Nielsen (1994) indicated that the infiltration process separates rain into two parts. One part is stored within the soil to supply water to the roots of vegetation and recharges ground water and second part is responsible for surface runoff. Expressions denoting rates of infiltration take the input rate of water or rainfall intensity and duration into account. Karanth (1987) found that the infiltration rate at any given time would attain the maximum value only as long as the input rate of water or in the case of rainfall intensity exceeds the infiltration rate. Groundwater is often an important contribution to stream flow especially when there is no runoff into the stream. Infiltration modelling approaches are often separated into three categories; physically based, approximate, and empirical models. A number of specific models have been developed for describing infiltration. Some of these models include Richard's, Green-Ampt, Horton, Philip and Kostiakov as shown below.

### 2.4.1 Richard Equation

Based on Richards (1931), the equation describes water flow in soils in terms of the hydraulic conductivity and the soil water pressure as functions of soil water content, for specified boundary conditions. The equation can be described as:

$$\frac{d\theta}{dt} = \frac{d}{dz}\left[ D(\theta)\frac{d\theta}{dz} \right] + \frac{dk}{dz}(\theta) \tag{2.12}$$

where;

$\theta$ = the water content ($m^3/m^3$)

$K$ = the hydraulic conductivity (m/day)

$z$ = the direction of flow rate (m)

Solving this equation is extremely difficult for many flow problems requiring detailed data input and use of numerical methods (Rawls,1993). Skaggs & Khaleel (1982) noted that numerical methods allow the hydrologist to quantify the vertical percolation of water. They also showed that numerical models were critical for assessment of groundwater recharge and in the analysis of contaminant movement through soil. However, numerical solutions are costly, data intensive, and time intensive computational procedures are required. Numerous field measurements have also to be made and therefore are rarely used in practice.

### 2.4.2 Green-Ampt Equation

The Green -Ampt infiltration method was developed to predict infiltration assuming that there will be excess water at the surface at all times (Chow *et al.*, 1998). The equation assumes that the soil profile is homogenous and the antecedent moisture content is uniformly distributed in the soil profile. As water infiltrates into the soil, the model assumes that the soil above the wetting front is completely saturated and there is a sharp break in moisture content at the wetting front. The Green-Ampt infiltration method is given as:

$$f = K\left[ 1 + \frac{(\phi - \theta_i)S_f}{F} \right] \tag{2.13}$$

where;

$f$ = the infiltration rate (cm/hr)

$K$ = the effective hydraulic conductivity (cm/hr)

$S_f$ = the effective suction in the wetting front (cm)

$\phi$ = the soil porosity (ratio)

$\theta_i$ = the water content (ratio)

$F$ = accumulated infiltration (cm)

To determine the amount of water entering the soil profile the difference between the amount of rainfall and the amount of surface runoff is obtained. The Green and Ampt infiltration method directly models infiltration, though it requires precipitation data in smaller time steps such as hours. However, accurate measurements may be limited due to heterogeneity in soil properties.

### 2.4.3 Philips Equation

The other method of determining infiltration rate is the Philip's method by ( Philip, 1954). It was derived from the theory of one dimensional infiltration and equations were developed which described the infiltration on both a short term and long term scale. It is based on the idea that when ponded infiltration in uniform soils occurs, the flow will approach the saturated hydraulic conductivity:

$$I = S\sqrt{t} + At \tag{2.14}$$

where; I = infiltration rate (cm/hr)

$S$ = sorptivity (m/s)

$A$ = the steady-state infiltration rate (cm/hr)

According to Philip (1957) , sorptivity is a measurable physical quantity that expresses the capacity of porous medium for capillary uptake and release of the liquid. The disadvantage of the method is that assumptions for which is applicable are rarely found in the field on large scale making the model not applicable for the present study.

### 2.4.4 Kostiakov Equation

The equation which was developed by Kostiakov (1932) and Lewis (1937) relates infiltration to time as a power function.

$$f_p = K_k t^{-\alpha} \tag{2.15}$$

where;

$f_p$ = the infiltration capacity in (cm/min)

$t$ = time after infiltration (min)

$K_k$ = constant (cm)

$\alpha$= constant (unit less)

$K_k$ and $\alpha$ depends on soil and initial conditions during the time of measurement. The main advantage of Kostiakov is that it is simple and easy to determine constants from measured

infiltration data. It gives a reasonable fit to infiltration data for many soils for over short time period (Clemmens, 1983). The model was not applied in this study because the study aimed at developing prediction equation for infiltration rate in different land use types.

### 2.4.5 Horton Equation

Horton's equation given by equation 2.16 is another viable option when measuring ground infiltration rates or volumes. It is an empirical formula that states that infiltration starts at a constant rate and decreases exponentially with time *t* (Horton, 1942). After some time, the soil saturation level reaches equilibrium where the rate of infiltration will level off.

$$f_t = f_c + (f_0 - f_c)e^{-kt} \tag{2.16}$$

where;

$f_t$ = infiltration rate at time t (cm/min)

$f_0$ = initial infiltration rate (cm/min)

$f_c$ = Constant infiltration rate at equilibrium (cm/min)

$k$ = A soil parameter per unit time that controls the rate of decrease of infiltration and depends on initial water content and application rate.

$t$ = time (min)

The main advantage of Horton's infiltration model is that it provides a good fit to data and assumes that infiltration capacity is not infinite at time zero but takes a finite value of $f_{o.}$ Hillel (1998) noted the model to be cumbersome in practice since it contains three constants that must be evaluated experimentally. Beven (2004) showed that the model neglected the role of capillary potential gradients in the decline of infiltration capacity over time. The model was used for this study to develop infiltration equations in different land use types since the parameters could be evaluated from the measured data.

### 2.4.6 Water Repellency

Water repellency (WR) is a property that has implications on the hydrologic balance in soils (Mataix-Solera *et al*., 2007). Seasonal variations in soil water repellency is influenced by different land use types (Gao *et al*., 2018). Persistent and spatial distribution of water repellency is a key factor controlling runoff dynamics and water availability in soil (Arcenegui *et al*., 2007). A study conducted by Arcenegui *et al*. (2007) on the immediate effects of wild fires on water repellency and aggregate stability in the Mediterranean calcareous showed that burning

increased the extent of water repellency. The author however did not consider the effect of other land use types like logging and agriculture.

### 2.5 Event-based Rainfall Partitioning

Rainfall partitioning by vegetation modifies the intensity of rain water that reaches the ground which in turn affect runoff generation (Charlier *et al.,* 2009). It was shown by Owens *et al.* (2006) that partitioning of gross rainfall into canopy interception , litter interception , stem flow and through fall allows estimation of physical impact of trees on local hydrologic budget. Interception (I) is defined as that portion of precipitation which is returned to the atmosphere through evaporation from the plant surface or absorbed by plant (Merriam *et al.*, 2017). Assuming direct evaporation of rain drops and wind drift are negligible, Interception loss is determined based on the correlation as in equation 2.17.

$$I = GR - TF - SF \tag{2.17}$$

where;

$I$ = Interception (mm)

$GR$ = Gross rainfall (mm)

$TF$ = through fall (mm)

$SF$= Stem flow (mm)

In Upper Njoro River Catchment, there are limited studies on quantification of rainfall partitioning yet reforestation is being exercised hence need for this study.

### 2.6 Frequency Analysis and Probability Distribution Models

Frequency analysis is important in finding the most suitable model that can be used to anticipate extreme events of any given phenomenon (Alam *et al.*, 2018). It is used to characterize extreme events in terms of magnitude, duration and frequency of occurrence by using probability distribution functions. The average length of time between events of the same magnitude or greater is referred to as return period. The methods of moments (MOM) estimators are used for parameter estimation of the probability distributions. Previous research by Mwetu (2010) who separated the effect of climate variability and land use effects on stream flow showed that land use changes were the major driving factor on the hydrologic response of Njoro River. Increased runoff rates and decreased infiltration rates have been reported through hydrological models.

Mwetu (2010) also observed that the stream flow in the catchment was stressed and was largely sustained by outflows from the shallow aquifers. Raude (2006) who also determined surface runoff and soil loss under varying rainfall intensity in selected land use practices in Njoro River catchment noted variations in flows .There is need to set the minimum flows recommended in order to protect the stream values. This can be achieved through frequency analysis of the extreme flows and their recurrence. The sample mean $\mu$, standard deviation $\sigma$ and coefficient of skewness $\gamma$ are the major parameters usually estimated by MOM and are calculated as shown respectively (Alam *et al*., 2018).

$$\overline{X} = \frac{1}{n}\sum_{i=1}^{n} x_i \tag{2.18}$$

$$\sigma = \sqrt{\frac{1}{n-1}\sum_{i=1}^{n}\left(x_i - \overline{x}\right)^2} \tag{2.19}$$

$$\gamma = \frac{n\sum_{i=1}^{n}\left(x_i - \overline{x}\right)^3}{(n-1)(n-2)S^3} \tag{2.20}$$

where; $\overline{X}$ = sample mean

$\sigma$ = standard deviation

$\gamma$ = coefficient of skewness

$n$ = number of observations in the data set

$i$ = observation number

$x_i$ = observation data

$S$ = Test statistic

The commonly used probability distributions include Normal, Log-normal, Pearson Type3, Log-Pearson Type3 (LP3), Gumbel, Generalized Extreme Value (GEV) and Generalized Pareto (GP).

### 2.6.1 Normal Probability Distribution

The Gaussian or normal distribution is commonly applied in the stream flow analysis and the two moments mean $\mu$, and variance $\sigma^2$ are the parameters of normal distribution (Alam *et al*., 2018). As indicated by Alam *et al*. (2018) and Friday & Runyi (2018), the probability density function (pdf) *f(x)* and the cumulative distribution function (cdf) *F(x)* for normal random variable is expressed as;

$$f(x)=\frac{1}{\sigma\sqrt{2\pi}}\exp\left[-\frac{1}{2\sigma^2}(x-\mu)^2\right] \tag{2.21}$$

$$F(x)=\frac{1}{\sigma\sqrt{2\pi}}\int_{-\infty}^{\infty}\left(\exp\left[\frac{1}{2\sigma^2}(x-\mu)^2\right]\right)dx \tag{2.22}$$

For the range of -∞ <x<∞.

### 2.6.2 Log-Normal Distribution

The pdf and cdf of the two parameter Log-normal (LN2) are expressed as shown below as indicated by Alam *et al*. (2018).

$$f(x)=\frac{1}{x\sigma_Y\sqrt{2\pi}}\exp\left[-\frac{1}{2\sigma^2{}_Y}(\ln(x)-\mu_Y)^2\right] \tag{2.23}$$

$$F(x)=\frac{1}{\sigma_Y\sqrt{2\pi}}\int_0^x\left(\frac{1}{x}\exp\left[-\frac{1}{2\sigma^2{}_Y}(\ln(x)-\mu_Y)^2\right]\right)dx \tag{2.24}$$

Where the range of random variables is *x>0*. The logarithm of *x* variable, *y= ln (x*) is well described by normal distribution. By using MOM estimators the two parameters are expressed as;

$$\sigma_Y=\left[\ln\left(1+\frac{\sigma_X{}^2}{\mu^2{}_X}\right)\right]^{\frac{1}{2}} \tag{2.25}$$

$$\mu_Y=\ln(\mu_x)-\frac{1}{2}\sigma^2Y \tag{2.26}$$

*Y*= Observations

Use of Log-normal involves transformation of data to logarithmic scale (Suhartanto *et al*., 2017). The model is applicable for fitting extreme rainfall events.

### 2.6.3 Pearson Type 3 (P3)

Pearson Type 3 (P3) is a 2-parameter Gamma distribution with a third parameter for the location. Bobee & Robitaille (1977) noted that P3 conforms generally to annual flood data. It is also suited in describing and estimating frequency and return period of hydrological drought (Sharma & Panu, 2014). The pdf and cdf functions are;

$$f(x)=\frac{1}{|\alpha|\Gamma(\beta)}\left[\left(\frac{x-\xi}{\alpha}\right)^{\beta-1}\exp\left(-\left(\frac{x-\xi}{\alpha}\right)\right)\right] \tag{2.27}$$

$$F(x)=\frac{1}{|\alpha|\Gamma(\beta)}\int_{\xi}^{x}\left[\left(\frac{x-\xi}{\alpha}\right)^{\beta-1}\exp\left(-\left(\frac{x-\xi}{\alpha}\right)\right)\right]dx \tag{2.28}$$

The parameters are shape $\beta$, scale $\alpha$ and location $\zeta$ which are estimated by MOM estimators as described in equations 2.29, 2.30 and 2.31 respectively.

$$\beta=\frac{4}{\gamma^2} \tag{2.29}$$

$$\alpha=\frac{\sigma_Y}{2} \tag{2.30}$$

$$\xi=\mu-\frac{2\sigma}{\gamma} \tag{2.31}$$

### 2.6.4 Log-Pearson Type 3

The Log-Pearson Type 3 (LP3) is also gamma family distribution describing a random variable whose logarithmic follows the P3 distribution. The pdf and cdf of LP3 as described by Alam *et al*. (2018) are as follows;

$$f(x)=\frac{1}{|\alpha|\Gamma(\beta)}\left[\left(\frac{\ln(x)-\xi}{\alpha}\right)^{\beta-1}\exp\left(-\left(\frac{\ln(x)-\xi}{\alpha}\right)\right)\right] \tag{2.32}$$

$$F(x)=\frac{1}{|\alpha|\Gamma(\beta)}\int_{0}^{x}\left[\left(\frac{\ln(x)-\xi}{\alpha}\right)^{\beta-1}\exp\left(-\left(\frac{\ln(x)-\xi}{\alpha}\right)\right)\right]dx \tag{2.33}$$

Amin *et al*. (2016) applied the model and found it to be the best fitting probability distribution model for annual maximum rainfall analysis in Pakistan.

### 2.6.5 Gumbel Distribution

The extreme value type 1 distribution also called the Gumbel distribution is often used to represent maximum processes. The corresponding pdf and cdf functions are;

$$f(x)=\frac{1}{\alpha}\exp\left[-\left(\frac{x-\beta}{\alpha}\right)-\exp\left(-\left(\frac{x-\beta}{\alpha}\right)\right)\right] \tag{2.34}$$

$$F(x)\exp\left[-\exp\left(-\frac{x-\beta}{\alpha}\right)\right] \tag{2.35}$$

The model was applied by Bhagat (2017) in Lower Mahi basin in India found it to be the best fitting for analysis of flood frequency. Gumbel distribution model was also found to be the best fitting model for peak discharges in Luvuvhu River Catchment in South Africa (Kundu *et al*., 2014).

### 2.6.6 Generalized Extreme Value (GEV) Distribution Model

The GEV model was applied by She *et al*. (2016) and found it to be suitable in frequency analysis of extreme dry spells during a rainy season in Wei River Basin. The equation used for estimation of extreme flow frequency at a desired return period was given as shown and was applied by Kundu *et al.* (2014).

$$Q_t = \mu + \left(\frac{\alpha}{k}\right)\left\{1-\left(-\log\left(\frac{T-1}{T}\right)\right)^k\right\} \tag{2.36}$$

where;

$T$= desired return period

$$\mu = \lambda_1 - \alpha\frac{\{1-\Gamma(1+k)\}}{k} \tag{2.37}$$

$$\alpha = \frac{\lambda_2 k}{(1-2^{-k})\Gamma(1+k)} \tag{2.38}$$

$$k = 7.8590 + 2.9554c^2 \tag{2.39}$$

$$c = \frac{2}{3+\tau_3} - \frac{\ln 2}{\ln 3} \tag{2.40}$$

where;

$\Gamma$ = Gamma function

$\tau$ = L-moment ratio

$\lambda_1$ and $\lambda_2$ = first and second L-moment approaches

### 2.6.7 Weibull Distribution Model

The extreme value type 3 distribution or W2 is often used for minimum stream flow as indicated by Alam *et al*. (2018).

$$f(x)=\left(\frac{k}{\alpha}\right)\left(\frac{x}{\alpha}\right)^{k-1}\exp\left[-\left(\frac{x}{\alpha}\right)^{k}\right] \tag{2.41}$$

$$F(x)=1-\exp\left[-\left(\frac{x}{\alpha}\right)^{k}\right] \tag{2.42}$$

With the range of x>0; α, k=0

The scale parameter $\alpha$ and the shape parameter $\beta$ are estimated using method of moments.

$$\mu=\alpha\,\Gamma\left(1+\frac{1}{k}\right) \tag{2.43}$$

$$\sigma^{2}=\alpha^{2}\left(\Gamma\left(1+\frac{2}{k}\right)-\left(\Gamma\left(1+\frac{1}{k}\right)\right)^{2}\right) \tag{2.44}$$

Assefa & Moges (2018) found Weibull distribution model to best fit low flow trends in Blue Nile Basin in Ethiopia.

### 2.6.8 Generalized Pareto

The Generalized Pareto distribution (GP) is useful for describing events which exceed a specified lower bound such as rainfall events above a given threshold (Alam *et al*., 2018). The three parameters are location ζ, scale α and shape k. The GP pdf and cdf are;

$$f(x)=\alpha^{-1}\exp\left[-(1-k)y\right] \tag{2.45}$$

$$y=-k^{-1}\log\left[1-k(x-\xi)\right],k\neq 0 \tag{2.46}$$

$$y=\frac{x-\xi}{\alpha};k=0 \tag{2.47}$$

$$F(x)=1-\exp(-y) \tag{2.48}$$

$$k=\left(\frac{1-3x_{3}}{1+3\tau_{3}}\right) \tag{2.49}$$

$$\alpha = (1+k)(2+k)\lambda_2 \tag{2.50}$$

The model was found to be suitable in frequency analysis of annual maximum flood in Segamat River Catchment (Romali & Yusop, 2017). In this research, different probability distribution models were tested and there performance compared using historical stream flow data. In addition, selection of the best fit probability distribution function for Njoro River at the gauging station 2FC05 was conducted and the best fit function was used to estimate peak flows for different return periods.

# CHAPTER THREE
# MATERIALS AND METHODS

## 3.1 Study Area

The focus of this research is on Upper Njoro River Catchment (UNRiC) which lies between Latitudes 0° 15' S and 0° 25' S and Longitudes 35° 50' E and 36° 05' E and is about 30 km$^2$. It lies between the Rongai-Njoro plains and the upper slopes of the Mau escarpment. The topography of the area is predominantly rolling land characterized by slopes ranging from 2% in the plains to 54% in the hills and elevation ranging from 2000- 3079 m above mean sea level. The catchment is drained by Njoro River which drains into Lake Nakuru.

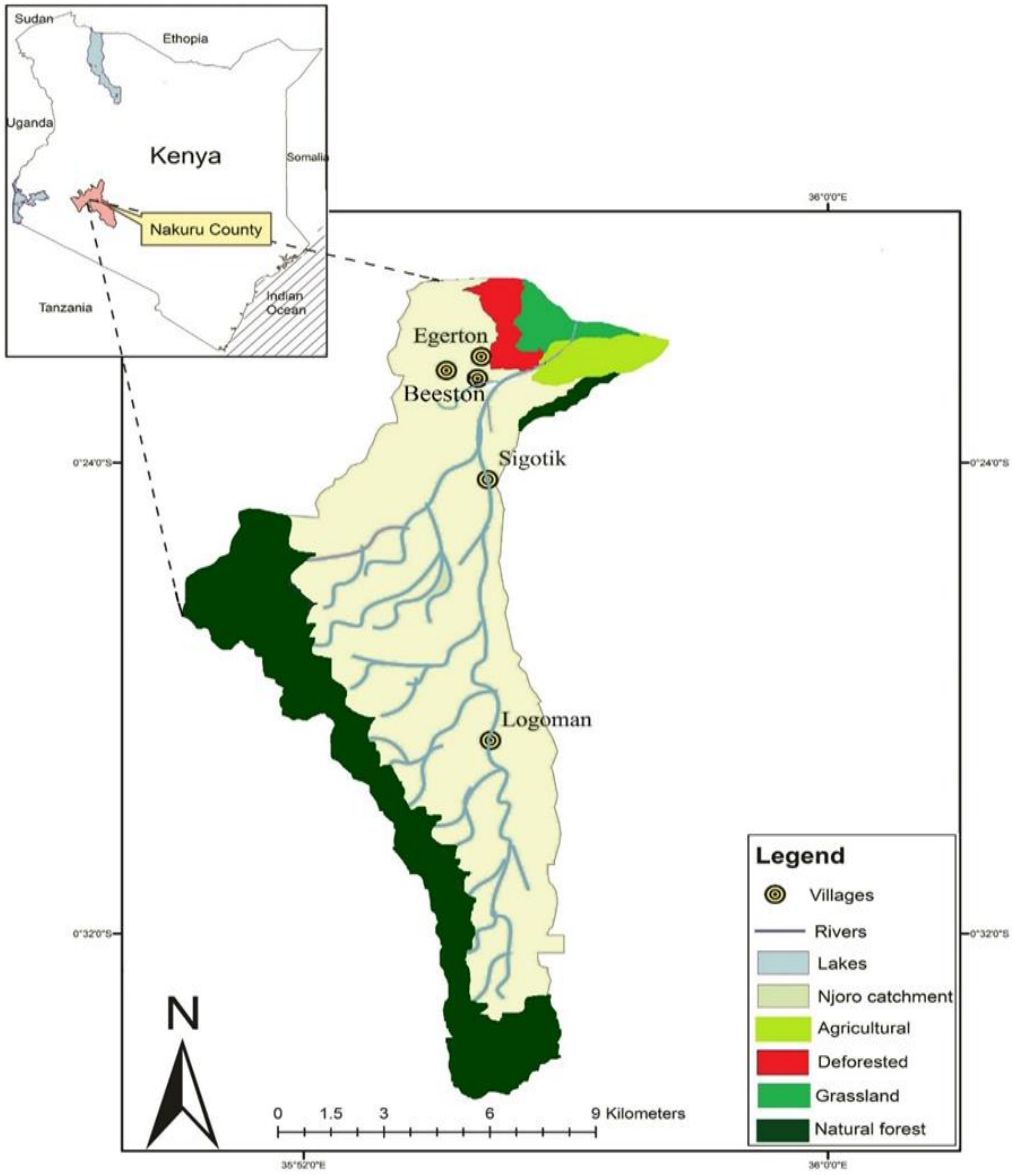


**Figure 3. 1:** Upper Njoro River Catchment

### 3.1.1 Climate

The average annual rainfall of UNRiC ranges from 840 mm to over 1200 mm. The mean monthly rainfall ranges from about 30 mm to over 120 mm with a trimodal pattern having peaks in April, August and November. The wettest months were April, May and August and November while the driest months were January and February. Minimum and maximum average monthly temperatures vary from 5 $^{o}$C to 28 $^{o}$C respectively. Meteorological data from Egerton weather station (ID. 9035092) from 1987 to 2016 showed that mean annual rainfall was 1073 mm and the air temperature was 21 $^{0}$C. The mean Pan Evaporation was 3.9 mm/day.

### 3.1.2 Description of the study plots

Experimental plots were established within the catchment whose location was purposely selected for different land use types as shown in Table 3.1.The locations were taken based on degrees decimal.

**Table 3. 1.** Location of the experimental plots.

| Latitude | Longitude | Land use type |
|---|---|---|
| -0.37 | 35.95 | Agricultural |
| -0.371 | 35.93 | |
| -0.371 | 35.93 | |
| -0.354 | 35.924 | Grassland |
| -0.367 | 35.924 | |
| -0.367 | 35.924 | |
| -0.37 | 35.92 | Deforested land |
| -0.355 | 35.92 | |
| -0.351 | 35.92 | |
| -0.36 | 35.93 | Natural forest |
| -0.364 | 35.93 | |
| -0.364 | 35.93 | |

Runoff plots were laid in the four land use types that included fallow agricultural land, natural forest, grassland and deforested land. Randomized Block Design (RBD) experimental design was used where land use types were blocked against the soil hydrologic response parameters. An area of 10 m by 3 m was set aside for the collection of runoff from the area.

### 3.2 Soil Hydrologic Response in Different Land Use Types

Land use type variations in soil properties such as bulk density, porosity, and soil texture, organic matter content and saturated hydraulic conductivity were determined as described in sub-sections 3.2.1 to 3.2.4. Event-based soil hydrologic response for different land use types was also evaluated in UNRiC. The soil hydrologic response parameters that were investigated included runoff volume and coefficients, water repellency, ponding time and infiltration rate.

#### 3.2.1 Bulk Density and Porosity

From each land use, three sites were selected where soil sampling was carried out at two soil depths of 0-15 cm and 15-30 cm. This is due to the spatial variations of soil properties in different land use types is significant with depth (Abegaz & Adugna, 2018). Soil samples used for bulk density determination were obtained using the core samplers. A soil core sampler was driven into the soil and was carefully removed to minimize any disturbance. The excess protruding soil on either side of the core was trimmed using a flat bladed knife. The core samples weighed, dried in the oven for 24 hours at a temperature of 105 $^{o}$C and their volume was calculated using the internal dimension of the core. The samples were taken four times during the field work period to examine the variations. Bulk density and porosity were obtained by the equation shown as applied by Utin & Oguike (2018).

$$\rho_b = \frac{m_s}{V_c} \tag{3.1}$$

where;

$\rho_b$ = Bulk density (g/cm$^3$)

$m_s$ = Mass of dry soil (g)

$V_c$ = Volume of the moisture can (cm$^3$)

Porosity was determined as in the equation;

$$\phi = 1 - \left( \frac{\rho_b}{\rho_s} \right) \tag{3.2}$$

where;

$\rho_s$ = Particle density = 2.65 g/cm$^3$

### 3.2.2 Soil Texture

Soil texture analysis was done in the soil laboratory using the hydrometer method (Bouyoucos, 1962). The air-dried soil from each experimental site was taken and 50 grams was weighed, put in the buffer cup and filled with distilled water. The resulting suspension was stirred for 15 minutes with an electric stirrer and then transferred in 1000 ml measuring cylinder. The cylinder was then filled to the 1000 ml mark with distilled water as shown in Appendix B.1. The suspension was agitated for five minutes and then a hydrometer calibrated to read grams per litre was inserted. The hydrometer and temperature readings were taken after 40 seconds and 2 hours. The percentage sand, silt and clay were computed as follows;

$$\%S_d = \frac{50 - C_{hr} \times 100}{50} \tag{3.3}$$

where; $S_d$ = Amount of sand content (%)

$C_{hr}$ = Corrected hydrometer reading after 40 seconds (g/L)

$$\%C_y = \frac{C_{hr} \times 100}{50} \tag{3.4}$$

where; $C_y$ = Amount of clay content (%)

$C_{hr}$ = Corrected hydrometer reading after 2 hours (g/L)

$$\%S_t = 100 - \left(\%S_d + \%C_y\right) \tag{3.5}$$

where;

$S_t$ = Silt content (%)

The USDA textural shown in Figure 3.2 was used to determine the soil texture class. The percent sand, clay and silt content were located on the textural triangle and the region where the three intersected was the soil textural class for the given soil.

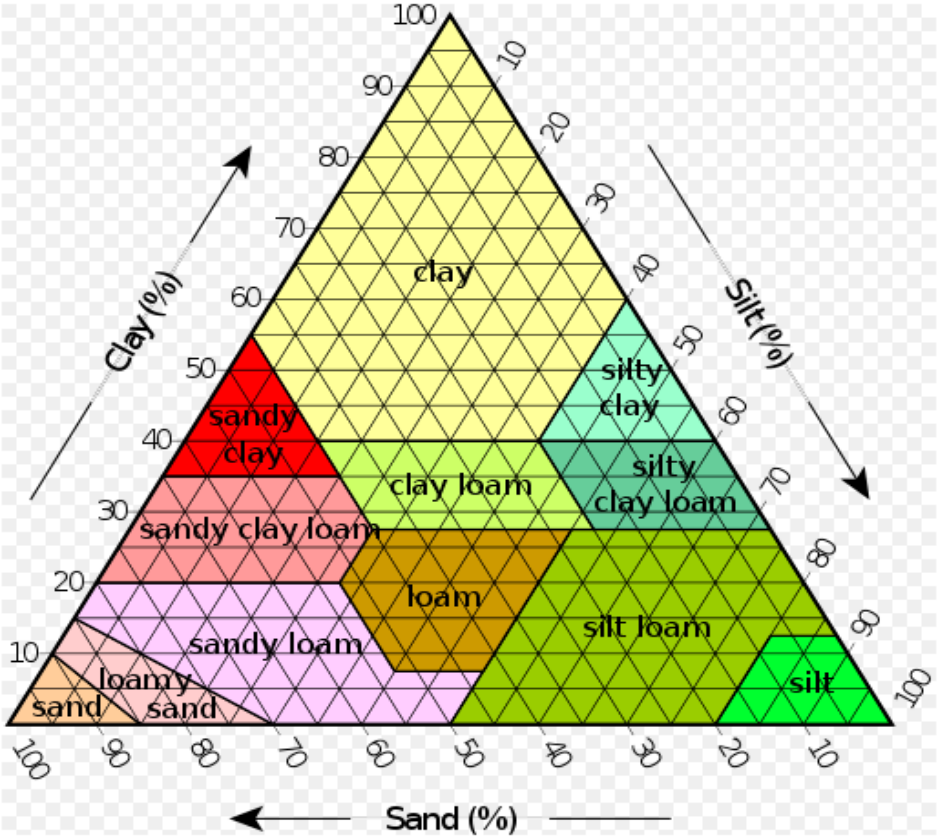


**Figure 3. 2:** Soil textural class triangle (Soil Survey Division Staff, 1993)

### 3.2.3 Soil Organic Matter

Soil organic matter was determined based on the Walkley-Black chromic acid wet oxidation method. A sample of soil from each land use site was sieved through a 0.5 mm sieve. The sample was then weighed and placed in a 250 ml conical flask where 5 ml of potassium dichromate ($K_2Cr_2O_7$) and 7.5 ml of conc. $H_2SO_4$ was added. The flask was then left in the fume chamber for 30 minutes after which it was quantitatively transferred to a 100 ml conical flask as shown in Appendix B.2. An indicator solution of 0.3ml ferrous ammonium sulphate was added until the color changed to greenish brown. A blank titration was also carried out. Percent organic carbon was calculated using the equation below:

$$\%OC = \frac{B_t - S_t \times n \times 0.003 \times f \times 100}{S_{wt}} \tag{3.6}$$

where;

$OC$ = Organic Carbon (g/kg)

$B_t$ = Blank titre

$S_t$ = Sample titre

$n$ = Amount of indicator solution

$f$ = Correction factor =2

$S_{wt}$ = Sample weight (g)

The value 0.003 was derived from the fact that 1 ml of 1.0 N $K_2Cr_2O_7$ is equal to 3.0 mg of carbon.

Based on Santra *et al*. (2018) who applied the pedotransfer function for soil water content prediction at FC and PWP, the function were developed from the multiple regression equation shown.

$$Y = a_0 + \sum_{k=1}^{k} a_k X_k \qquad (3.7)$$

where;

$Y$= dependent variable (moisture content at FC and PWP)

$X_k$ = $k^{th}$ independent variable

$a_0 ...., a_k$ = Regression coefficients

k = Number of independent variables.

The major soil properties incorporated in the multiple regression equation included sand content (%), clay content (%) and organic carbon content (g/kg).

### 3.2.4 Saturated Hydraulic Conductivity

Saturated hydraulic conductivity was determined in the laboratory using the constant head permeameter method for soil samples from the four land use types. The soil sample was placed in the permeameter and water was passed through as shown in Figure 3.3. The inflow fluid was maintained at a constant head *(h)* above the datum and outflow *(Q)* was measured as a function of time.

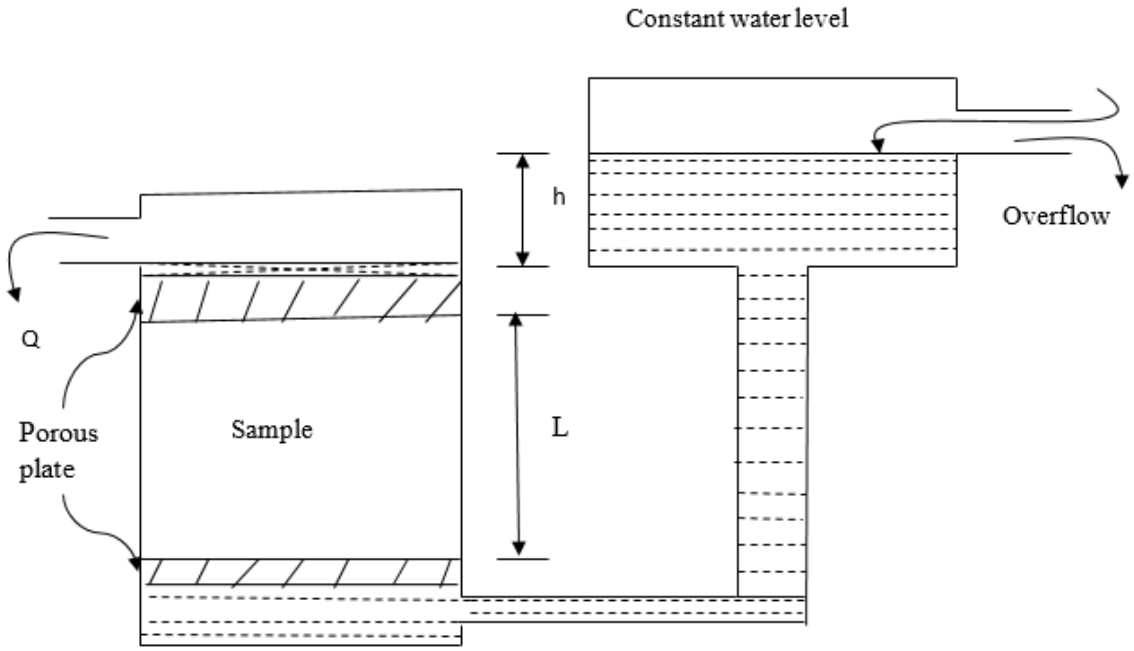


**Figure 3. 3:** Constant head method

Darcy's law as applied by Santra *et al*. (2018) was used to determine the saturated hydraulic conductivity after an outflow rate using the following relation.

$$K = \frac{QL}{hA} \tag{3.8}$$

where;

$Q$ = Outflow ($m^3/s$)

$K$ = hydraulic conductivity (cm/s)

$L$= Length of sample (cm)

$A$ = Cross-section area of sample ($cm^2$)

$h$ = fluid head difference (cm)

### 3.2.5 Runoff Collection and Sampling

Experimental plots were established within the catchment whose location is as shown in Table 3.1. Runoff plots were laid in the four land use types that included fallow agricultural land, natural forest, grassland and deforested land.

Each runoff plot measured 10 m long and 3 m wide as shown in Figure 3.4 and had a uniform slope of 10 % which was established using a line level and level boards. The runoff volume is dependent on the degradation process of the land as compared to runoff plot size (Moreno-de las Heras *et al*., 2010). The plots were reinforced with dump proof course (DPC) to prevent external runoff from entering the plots. Plot runoff was directed into a collection bucket of capacity 17 L .The collection containers were checked after every rainfall event and the amount of runoff was measured and recorded. Runoff was expressed as water depth in (mm). Runoff coefficients were calculated as the ratio of runoff depth to rainfall depth.

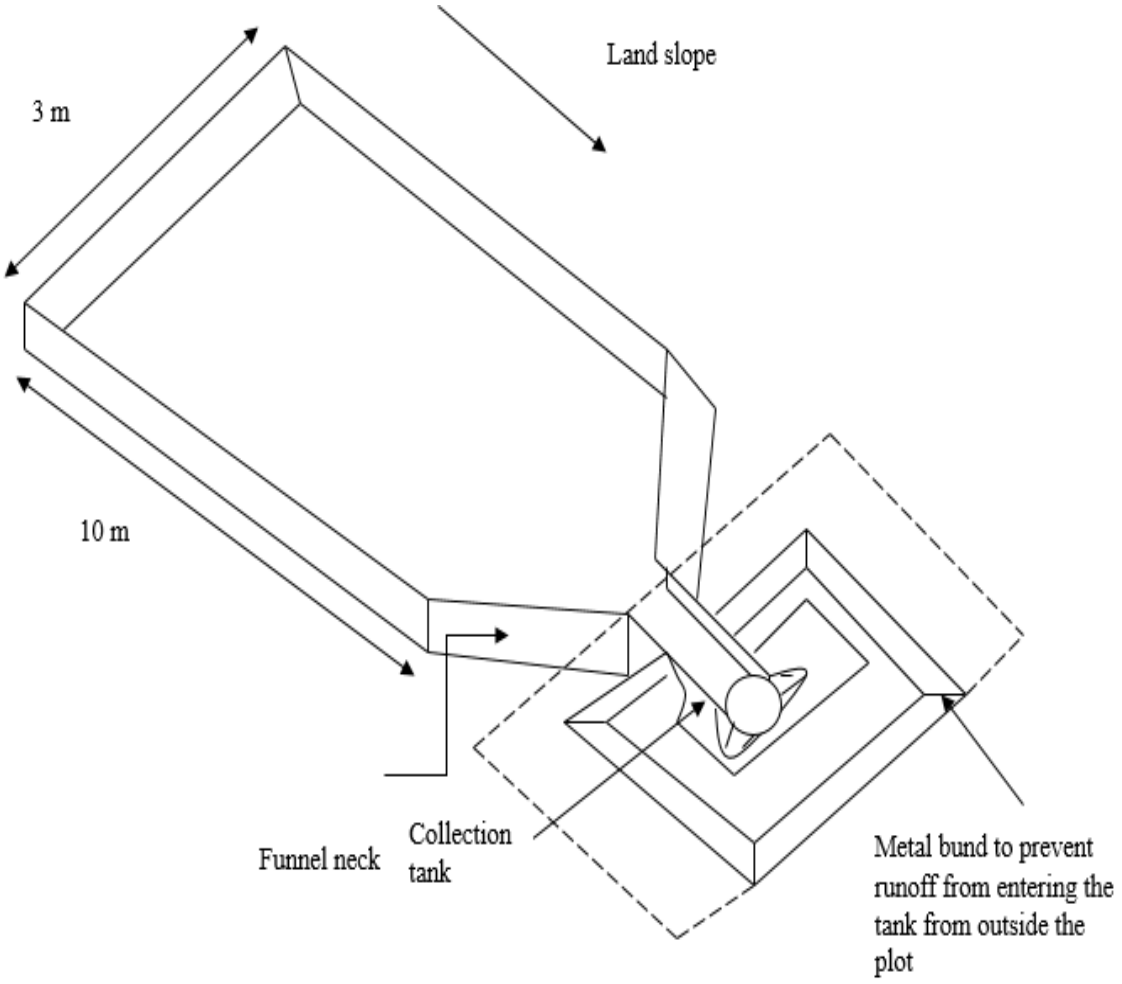


**Figure 3. 4:** Layout of runoff plots

### 3.2.6 Water Repellency

Water repellency was used as an indicator of the ability of soil to resist penetration of water. It has an implication on hydrologic balance in soils and was measured using water drop penetration time (WDPT) method as described by Van't Woudt (1969). Litter was removed

from the surface and then the surface was smoothed to make it homogenous. Five drops of distilled water were placed in different points of the soil surface and the time of infiltration was recorded. The water repellency values that were obtained with WDPT were classified according to the classification by Doerr *et al.* (2006) as shown in Table 3.2. The tests were carried out early in the morning when humidity was high to reduce the effect of evaporation.

**Table 3. 2:** Water drop penetration time classification

| Penetration time | Class |
|---|---|
| Less than 1 second | Not significant |
| 1-10 seconds | Very low |
| 10-50 seconds | Low |
| 50-260 seconds | Moderate |
| Greater than 260 seconds | Moderate to severe. |

**Source:** Doerr *et al.* (2006)

### 3.2.7 Ponding Time

Ponding time for different land use type under uniform rainfall intensity was determined using the direct method (Assouline *et al.*, 2007). The following steps were used to evaluate ponding time. Before ponding is achieved the expression that applies is as below. Ponding was based and 82 minute storm that was recorded during the field work period.

$$F(t) = R(t) \ for\, t \le t_p \tag{3.9}$$

where;

$F_{(t)}$ = Cumulative infiltration (cm) at time t (min)

$R_{(t)}$ = Rainfall depth (cm) at time t (min)

$t_p$ = ponding time (min)

Based on Brutsaert (2005) , the post ponding infiltration rate was given by the equation:

$$f_{(F)} = f_{cap_{(F_{cap})}} \ for\ t = t_p \tag{3.10}$$

where;

$f_{(F)}$ = Post ponding infiltration rate (cm/min)

$f_{(cap)F(cap)}$ = infiltration capacity (cm/min)

Therefore, t at the moment when ponding occurs;

$$r(R) = f(F) = f_{cap}\left(F_{cap}\right) at\ t = t_p \quad (3.11)$$

Therefore ponding was the time when;

$$r(R) = f_{cap}\left(F_{cap}\right) \text{ was fulfilled.} \quad (3.12)$$

Graphical plots of rainfall intensity versus cumulative infiltration and infiltration capacity were made in the same space. The point where the plots were intersecting denoted the time of ponding. Inverse function of cumulative rainfall versus time was plotted and then was translated to determine ponding time in different land use types.

### 3.2.8 Infiltration Rate

In-situ measurements of infiltration rate of the soil were done by a double ring infiltrometer. Tests were carried out four times in each of the four land use types. The inner ring had a diameter of 28.5 cm while the outer ring had a diameter of 53 cm. The rings were driven into the soil to a depth of about 5 cm below the soil surface using a metal plate and a sledge hammer. Water was filled to 20 cm above the soil surface in both rings and the level was maintained by adding water up to the mark. The inner ring was maintained at the 20cm head level and the amount of water used to top up was recorded at; 2, 5, 10, 15 25, 45 and 60 minutes. Tests were carried out for one hour because preliminary trials showed that at 1 hour, infiltration capacity had been reached. Cumulative depth of infiltration was then computed for each land use type.

### 3.2.9 Horton Prediction Equation

The Horton equation for predicting infiltration was determined from the field experiments in the four land use types. The field collected infiltration data was used to determine the constant of Horton's equation. The equation assumes that infiltration capacity is not infinite at time zero but takes a finite value as indicated by Horton (1942) and is given by;

$$f = f_c + (f_0 - f_c)e^{-kt} \quad (3.13)$$

The constants $f_0$, $fc$ and $k$ were found by taking natural logarithm on both sides of the equation.

$$\ln(f - f_c) = \ln(f_0 - f_c) - kt \quad (3.14)$$

Letting $y$ to denote $ln\ (f\text{-}f_c)$ and $c$ to denote $ln\ (f_0\text{-}f_c)$

Therefore equation 3.14 reduces to:

$$y = c - kt \quad (3.15)$$

where ;

y= infiltration rate (cm/min)

k= decay constant

t = Time (min)

A graph of *y* and *t* was then plotted and a straight line was fitted. The slope of the line defined the value of *k* while the intercept on the y-axis gave the value of *c*. The value of $f_c$ for each case was obtained from field measured data.

### 3.3 Determination of Event-based Rainfall Partitioning

Measurements were carried out in the planted forest on a plot of size 0.24 ha at 35.924 $^0$E and 0.367 $^0$S and 2265 m above sea level from October to December 2017. The tree species selected in the area were Red stinkwood since it was the most dominant species hence could impact soil hydrological functioning. The means tree height and diameter at breast height (DBH) was 5 m and 32.8 cm respectively. Gross rainfall (GR) was collected within the study area using rain gauges located in the nearby weather recording station at Egerton University (9035092). In the experimental plot through fall and stem flow were measured from six trees by capturing the water using a polythene sheet as shown in Appendix B.5.

The through fall (TF) and stem flow were collected in 20 L containers and the volume was measured using a graduated cylinder with an accuracy of 1ml after an event had occurred. In the situations where the events extended into the night the measurement was done in the morning. To determine the throughfall and stem flow depth, crown projection area was obtained. The crown radius which was measured based on Ahmadi *et al.* (2009) to be the distance from the centre of the tree stem to the edge of the crown. It was measured using a straight edge and a tape measure. The corresponding through flow and stem flow depth of each tree was determined by dividing volume collected by crown cross section area. Interception loss (I) was defined as that portion of precipitation which was returned to the atmosphere though evaporation from the plant surface or absorbed by plant (Merriam *et al.*, 2017). Interception was determined using the following equation:

$$I = GR - TF - SF \quad (3.16)$$

where;

$I$ = Interception l (mm)

$GR$ = Gross rainfall (mm)

$TF$ = through fall (mm)

$SF$ = Stem flow (mm)

Net precipitation was also determined through the equation;

$$NR = GR - I \quad (3.17)$$

where;

$NR$ = net rainfall (mm)

$I$ = Interception (mm)

$GR$ = Gross rainfall (mm)

### 3.4 Probability Distribution Models

#### 3.4.1 Selection of best fitting probability function

The magnitude of peak flows was predicted using return period and probability functions. Stream flow data was obtained from Water Resources Authority (WRA), Nakuru for the two gauging stations that included Egerton (ID.2FC05) and Shuru tributary (ID.2FC11). Data from gauging station at the Egerton Bridge (ID.2FC05) was used in this study since it had long record of consistent data, less missing records and is functional. The duration of data used was from 1970 July to 2018. Annual monthly peak discharges series were extracted for each hydrological year. A probability plot was used for assessing the distributions to select the one which provided the best fit. The Easyfit 5.6 Professional software was used to analyze the peak flow frequency within the catchment for different probability distribution models.

#### 3.4.2 Goodness of Fit Test

The probability distribution functions were ranked based on Kolmogorov Smirnov and Chi-squared goodness of fit models (Friday & Runyi, 2014). The equations are shown respectively as:

Kolmogorov-Smirnov function;

$$D_n = Sup_x \left| F_n(x) - F(x) \right| \quad (3.18)$$

where;

$D_n$ = Kolmogorov-Smirnov statistic

$Sup_x$ = Least Upper Boundary

$F_n(x)$ = Cumulative density function of hypothesized distribution

$F(x)$ = Empirical distribution function of the observed

Chi-squared function;

$$x^2 = \sum_i^n \left[ \frac{O_i - E_i}{E_i} \right]^2 \tag{3.19}$$

where;

$x^2$ = Chi-square test statistic

$O_i$ = Observed frequency

$E_i$ = expected frequency

$n$ = Sample size

The best fitting probability distribution models were used to estimate peak discharges for Njoro River at 2FC05 for the return periods of 2, 5, 10, 25, 50, 100 and 200 years.

# CHAPTER FOUR

# RESULTS AND DISCUSSION

## 4.1 Soil Hydrologic Response for Different Land Use Types

The soil properties that included bulk density, porosity, soil texture, organic matter content and saturated hydraulic conductivity (Ksat) were determined in different land use types .The key parameters of soil hydrologic response that included the infiltration capacity, runoff volume, water repellency and ponding time were also determined.

### 4.1.1 Variation in Soil Properties

Four sets of soil properties measured at depth of 0-15 cm and 15-30 cm were determined in the natural forest, grass land, fallow agricultural land and deforested areas to determine variations of $K_{sat}$ with land use type for the period of September to December 2017. Figure 4.1 showed monthly variations in saturated hydraulic conductivity under different land use types.

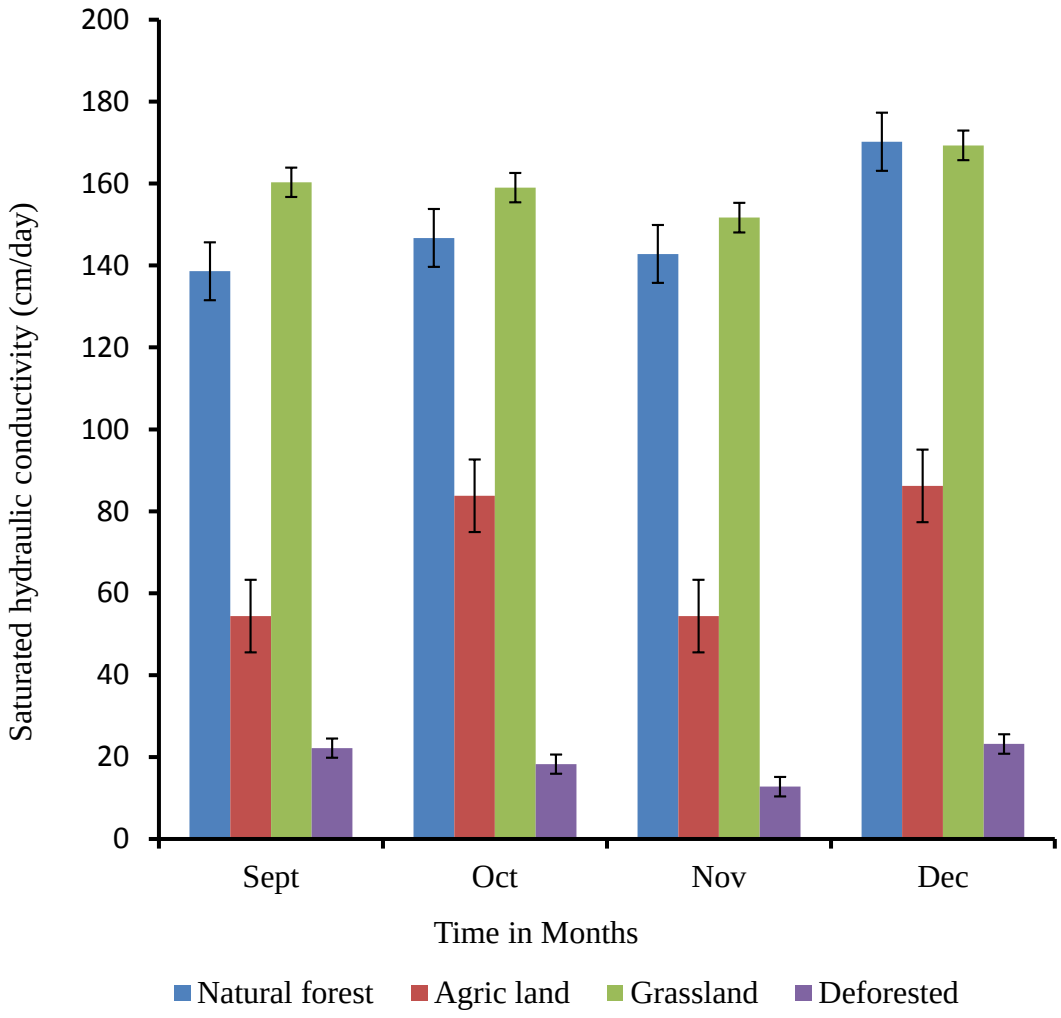


**Figure 4. 1**: Variations in $K_{sat}$ with time

Based on Figure 4.1, soil water content was a factor explaining the variations in saturated hydraulic conductivity with time and rainfall contributes to amount of water in the soil. There was significance difference in Ksat between November and December as indicted by the error bars. Saturated hydraulic conductivity was highest during September and December for all land use types .This is attributed to the low amounts of rainfall during this moths hence increase in hydraulically active pores. Reduced saturated hydraulic conductivity was observed during months of October and November which had gross rainfall of 134.2 mm and 112.9 mm respectively. This is due to cumulative effect of gravity and rainfall hence reduction in porosity. The findings are in agreement with Schwen *et al.* (2011) who carried out a study on the temporal dynamics of soil hydraulic properties and water-conducting porosity and found soil water content variation to be the main factor contributing to variation of $K_{sat}$ at different times. Amer *et al*. (2014) also noted that dispersion and migration of colloidal particles and subsequently lodging in the soil pores lead to reduction in saturated hydraulic conductivity of a given soil. Figure 4.2 shows the variations in bulk density at different times of the field work.

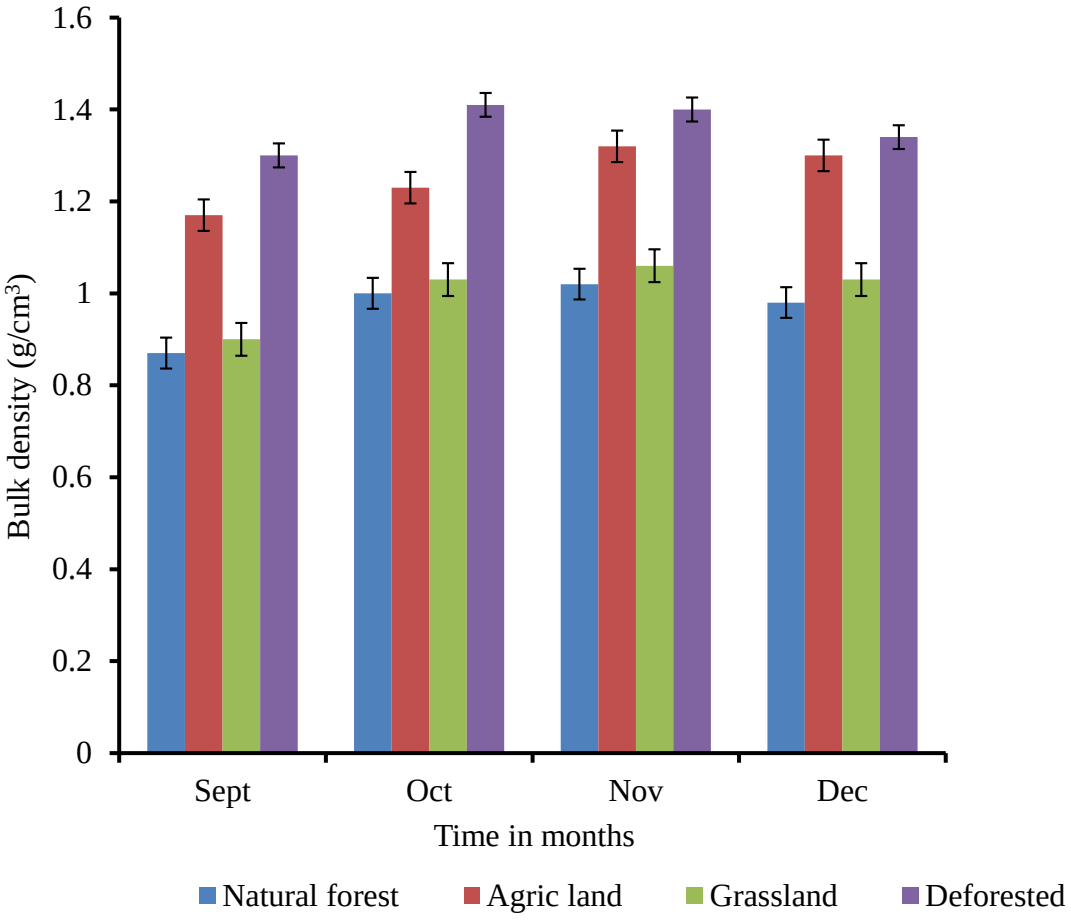


**Figure 4. 2:** Variations in bulk density with time in months

Based on the results in Figure 4.2, there were significant variations from the four sets of data collected in September, October, November and December as indicated by error bars. The month of December had the lowest value of bulk density. This could be due to low soil water content during the month hence high porosity. High values of bulk density were observed during the month of October. The high values could be associated to limited interception of the heavy rainfall that was experienced during the month hence causing compaction in soils due to high terminal velocity of the raindrops. This concur with Assouline (2004) who argued that rainfall impact on bare soils can result in rainfall-induced surface sealing hence causing low infiltration rates. The results also concur with the findings of Alletto & Coquet (2009) who found that time was the most important source of bulk density variability for surface and subsurface conditions as a result of moisture variation.

### 4.1.2 Effect of Different Land Use Types on Soil Properties

The soil hydrological parameters were analyzed to characterize the field experimental areas. These included soil bulk density (BD), porosity, saturated hydraulic conductivity ($K_{sat}$) and soil organic matter content (SOM). Figure 4.3 presented the soil properties for the land use types.

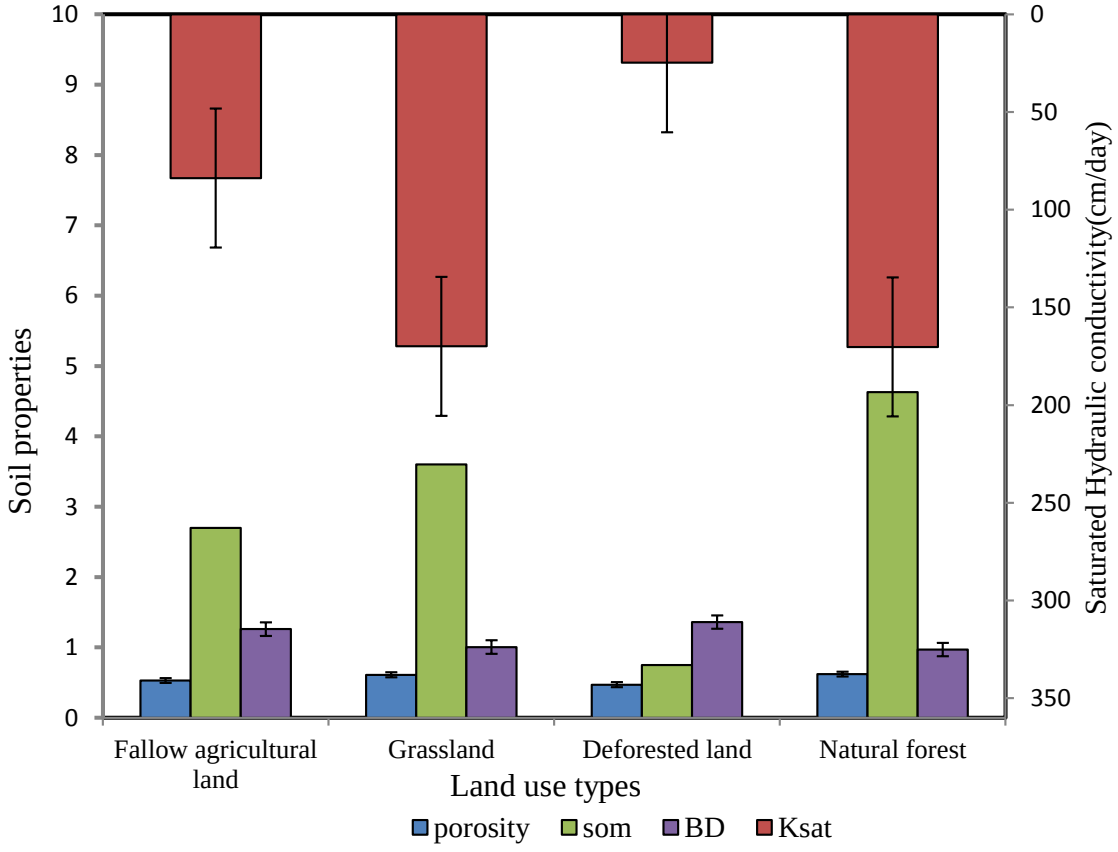


**Figure 4. 3**: Soil properties for different land use types

Based on Figure 4.3, it was observed that the highest value of bulk density was in the deforested land while the lowest value was in the natural forest. The mean values of bulk density ranged from 0.97 to 1.36 g/cm$^3$. The high bulk density in deforested land could be attributed to soil compaction during deforestation. The lower bulk density in the natural forest could be due to high percentage of macro-pores generated by root channels and presence of duff and O-horizon materials. The results are consistent with the findings of Yimer *et al*. (2008) where bulk density in different land use types was analyzed. They found that bulk density in indigenous forest was lowest as compared to other land use types. Porosity was found to be highest in the natural forest as compared to the other land use types. The high porosity in the natural forest could be due to the coarseness of the soil structure hence more pore spaces. The findings concur with dos Santos *et al*. (2018) who observed lower bulk densities and higher porosity in the natural forest as compared to the other land use types.

Saturated hydraulic conductivity was found to be 170.21, 169.93, 83.80 and 24.78 cm/day in the natural forest, grassland, fallow agricultural land and deforested land respectively as shown in Figure 4.3. Saturated hydraulic conductivity ($K_{sat}$) was the highest in the natural forest land and decreased in the order of grassland, fallow agricultural land and deforested land respectively. The findings concur with Zwartendijk *et al*. (2017) who examined saturated hydraulic conductivity in natural forest and deforested land and found out that $K_{sat}$ in forest to be higher than deforested land. Correlation tests were carried out between saturated hydraulic conductivity and the other soil properties to determine how each property related with $K_{sat}$. There was significant negative correlation (-0.98) between saturated hydraulic conductivity and the bulk density. The correlation coefficient between $K_{sat}$ and porosity, soil organic matter content, and moisture content at field capacity were 0.998, 0.960, and 0.997 respectively. Through ANOVA there were significant differences between plots in the different land use types at 95% level of significance.

The organic matter content was found to be 4.63% in the natural forest, 2.70% in the agricultural land that had been left fallow, 3.60% in the grassland and 0.75% in the deforested area. The natural forest had the highest organic matter content while the deforested area had the lowest organic matter content. This could be attributed to the dense canopy that drop high amount of litter in the natural forest which decomposes to add on the organic matter. The findings are in line with Tilahun & Asefa (2009) who carried out a study on soil organic matter

contents in four land use systems: forestland, grassland, fallow land and cultivated land and found the carbon content to be highest in forest.

Soil texture analysis was carried out in the soil laboratory for the 27 soil samples from the 12 sites using hydrometer method were presented as in Figure 4 .4.

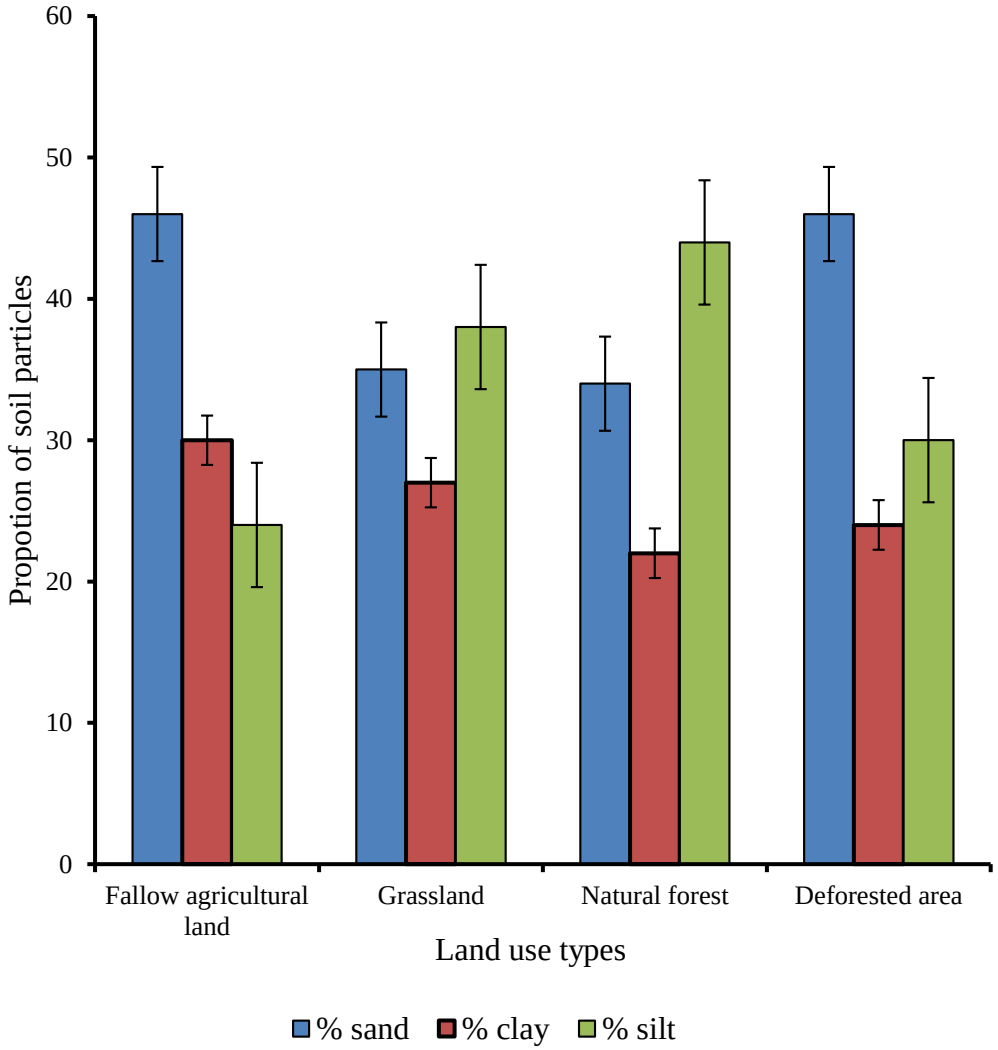


**Figure 4. 4:** Soil particle proportions for different land use types

The clay content of the samples ranged from 22 to 38 %, silt ranged from 24 to 44 % and the sand content between 34 to 46%. The sand content was highest in the deforested land and fallow agricultural land. Analysis of variance of the particle proportions showed that sand, silt and clay content had a $p$ <0.05 hence significantly different for the four land use classes ($p$ = 0.04). Based on USDA textural triangle, the soil classes were sandy clay loam, clay loam and loam in the fallow agricultural land, grassland and natural forest respectively. The pedotransfer

function developed to predict soil water content at field capacity and permanent wilting point within the catchment are as shown.

$$\theta_{FC} = -0.15C + 2.03OC + 0.12S \quad (4.1)$$

$$\theta_{PWP} = -1.6\times10^{-5}C + 0.000204OC + 0.12\times10^{-5}S \quad (4.2)$$

where;

$\theta_{FC}$ = moisture content at field capacity (%)

$\theta_{PWP}$ = Moisture content at permanent wilting point (%)

$C$ = Clay content (%)

$OC$ = Organic carbon content (g/kg)

$S$ =Sand content (%)

### 4.1.3 Infiltration Capacity

The cumulative depth of infiltration was computed for each land use and was as shown in Figure 4.5.

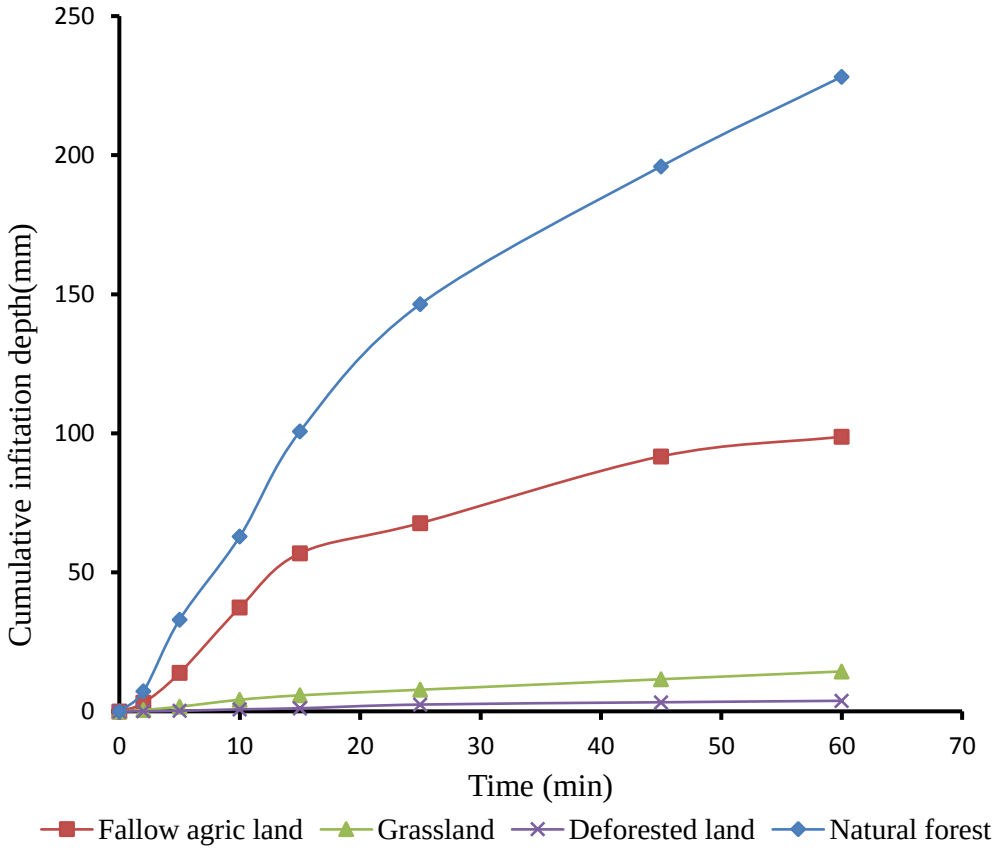


**Figure 4. 5**: Cumulative infiltration for different land use types

There were significant differences in infiltration rates and cumulative infiltration between the land use types ($p$ = 0.004) at 0.05 level of confidence. The infiltration capacity was highest in the natural forest and lowest in the deforested land. The reduction in the infiltration rate in deforestated land was attributed to the compaction and soil structural degradation during logging and human activities in the forest. The soil structural degradation consequently led to reduction in macropores and inconsitency in pore space on the sub surface soil hence reduction in infiltration rate and increase in surface runoff. The changes in infiltration capacity in turn changed the pathways that water took towards the stream and therefore stream flow response to rainfall and water quality changed (Bruijnzeel, 2004). A study conducted by Yimer *et al.* (2008) on effects of different land use types on infiltration capacity in a catchment in the highlands of Ethiopia found that changes in infiltration capacity were attributed to land use change rather than location and slope which is consistent with the present findings. Beyond 60 minutes the infiltration capacity of the soils was achieved and the curve flattens. This implies beyond this level the ponding takes place hence runoff generation.

### 4.1.4 Soil Hydrologic Response

The cumulative runoff was plotted against cumulative rainfall as in Figure 4.6.

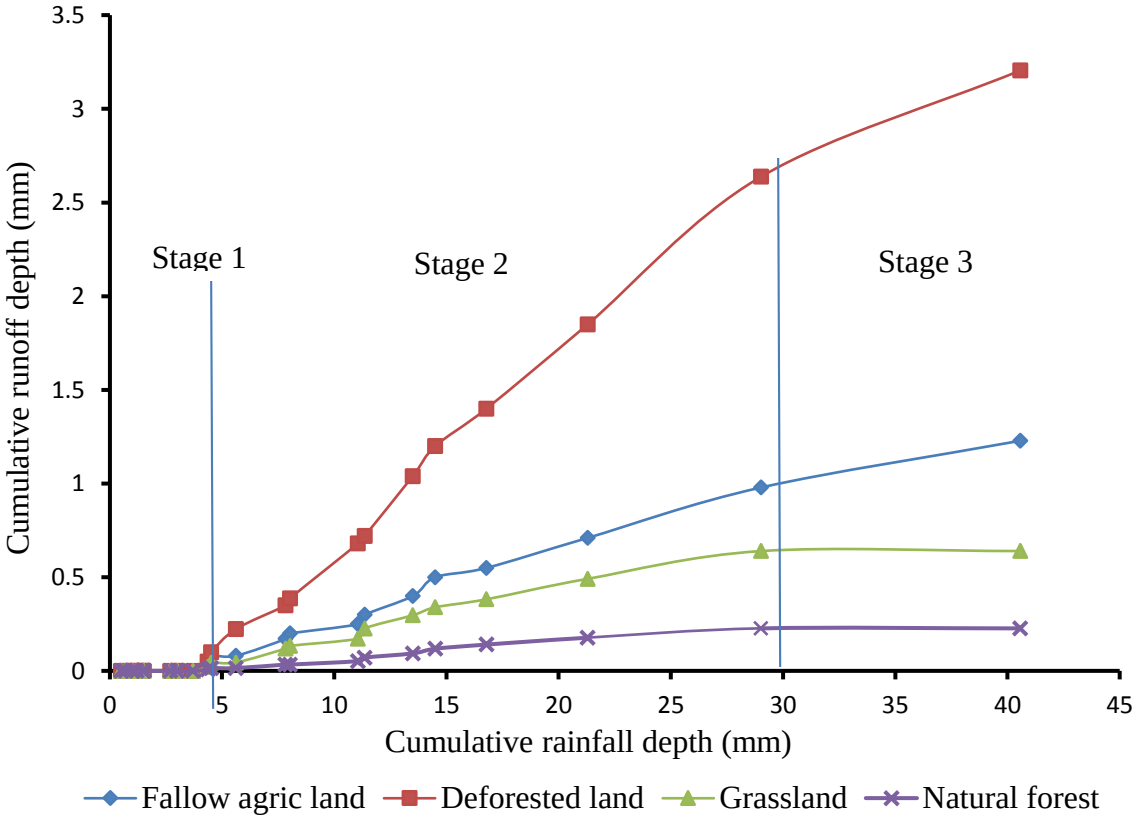


**Figure 4. 6:** Soil hydrologic response for different land use types

From the plot in Figure 4.6, there were three distinct stages in the rainfall-infiltration and runoff processes. The first stage was from the start of rainfall to the initiation of runoff where all the rainfall infiltrates. The second stage was when infiltration and runoff occurred at the same time. At this point there was an almost linear relationship which indicates that there is constant infiltration rate. Stage three represent scenarios when all the rainfall was being converted to runoff hence rainfall being equal to runoff. The curves display almost the same pattern although infiltration rates were higher in the natural forests as compared to other land use types hence making runoff to take long to start. The curves also depict that reduction in infiltration began almost at the same time although the amount varied in different land use types. At the beginning of the rainy season the soil was drier thus higher storage capacity and thus infiltration rate was high. Coefficients were calculated by expressing the runoff as a proportion of rainfall and the average coefficient ranged from 0.0077 to 0.0006 with deforest land having the highest while natural forest having the lowest. As indicted by Tilahun *et al.* (2013) an increase in runoff coefficient shows low infiltration and high runoff. High runoff rates in deforested areas are due to degraded soil structure disturbance during deforestation thus changing the flow paths of water (Winkler *et al.*, 2010).

### 4.1.5 Horton Prediction Equations

Horton's equation describing data in various land use type was developed through regression analysis. The infiltration capacity values for each land use were obtained from the infiltration rate curves. The equations that were developed are as in Table 4.1.

**Table 4. 1:** Modified Horton's equation for different land use types

| Land use | Equation | Equation Number. |
|---|---|---|
| Natural forest | $f = 100 + 800.96e^{-2.81t}$ | 4.3 |
| Fallow agricultural land | $f = 20 + 4.58e^{-2.84t}$ | 4.4 |
| Grassland | $f = 10 + 0.8e^{-0.88t}$ | 4.5 |
| Deforested land | $f = 2 + 1.76e^{-0.98t}$ | 4.6 |

These models can be applied to other similar land use types where tests have not been conducted or to check the accuracy and reliability of automated systems at defined intervals.

### 4.1.6 Water Repellency

Water repellency (WR) was determined in the four land use types using water drop penetration time (WDPT) method. The results were as shown in Figure 4.7.

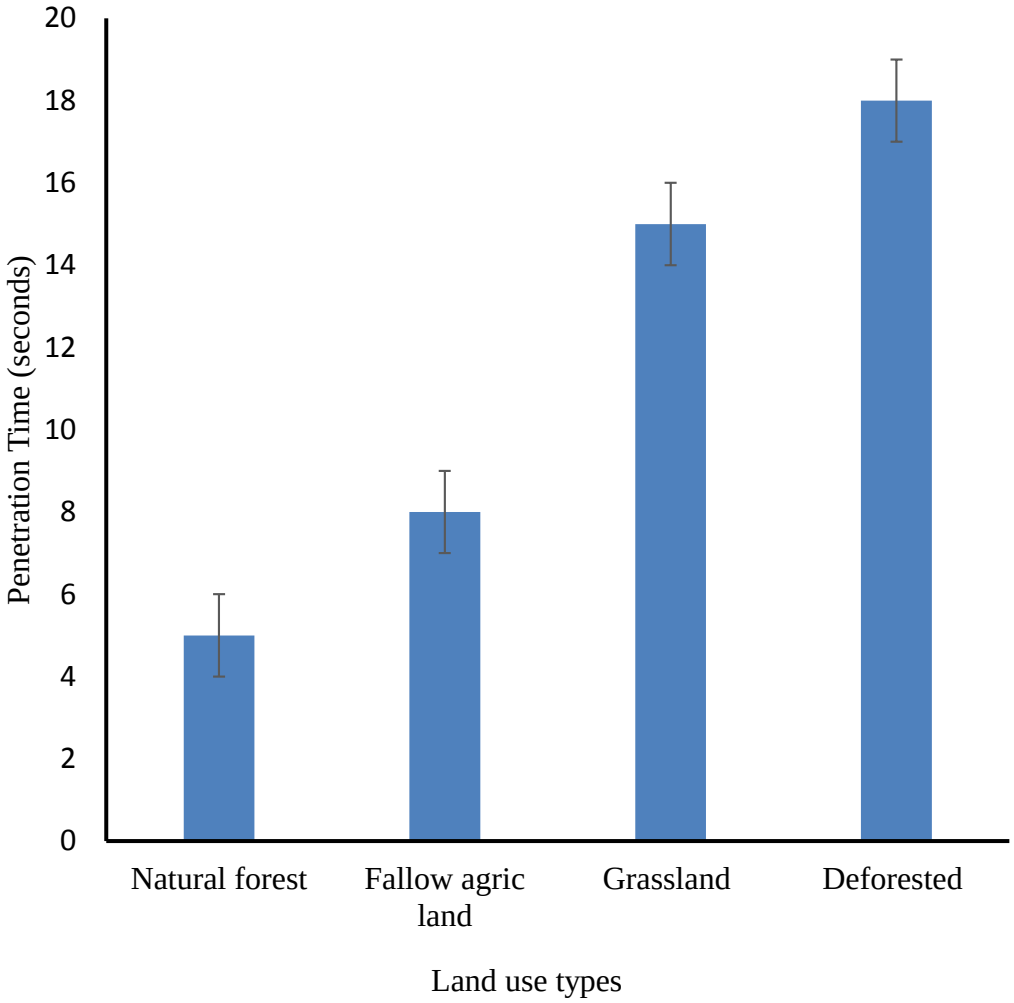


**Figure 4. 7:** Penetration Time in different land use types

The results in Figure 4.7 showed that water repellency was not significantly different in fallow agricultural land and natural forest as indicted by the error bars. However, there was significant different for water repellency for natural forest and deforested land where the deforested land has the highest penetration time. The soils in the deforested land were found to be the most water repellent hence resulting into faster ponding and runoff generation. This also is the evidence of the high runoff and low infiltration rates experienced. Observation by Cerda *et al.*, (2007) showed that low vegetation cover deteriorates the soil structure due to compaction is responsible for the high soil water repellency in deforested land. Slight repellency in soils has

a substantial effect on infiltration rates hence increase in runoff generation especially for dry soils

### 4.1.7 Ponding Time

The response of ponding time in different land use types was tested under varying rainfall intensity. The relationship between cumulative rainfall intensity, cumulative infiltration capacity and cumulative infiltration depth were as shown in the Figure 4.8.

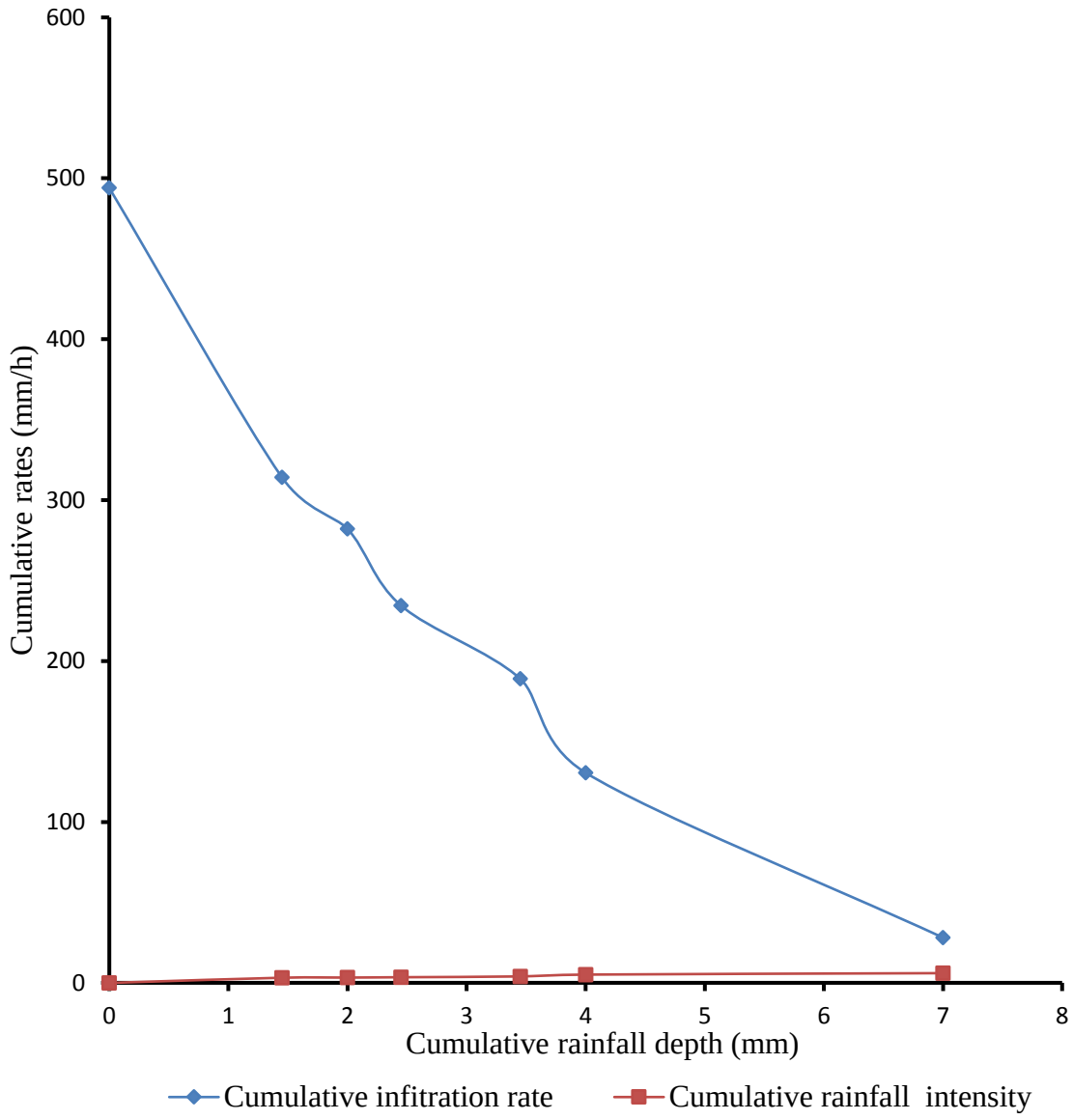


**Figure 4.8:** Ponding in fallow agricultural land

The Figure 4.8 showed that ponding could not be realized for the 82 minutes storm. This explains the low runoff rates and high infiltration that were experienced. Results showed that under the same varying intensity the infiltration rate was almost equal to the rainfall intensity

hence ponding took a slightly longer time. Figure 4.9 represented the relationship of cumulative infiltration and rainfall intensity in the natural forest.

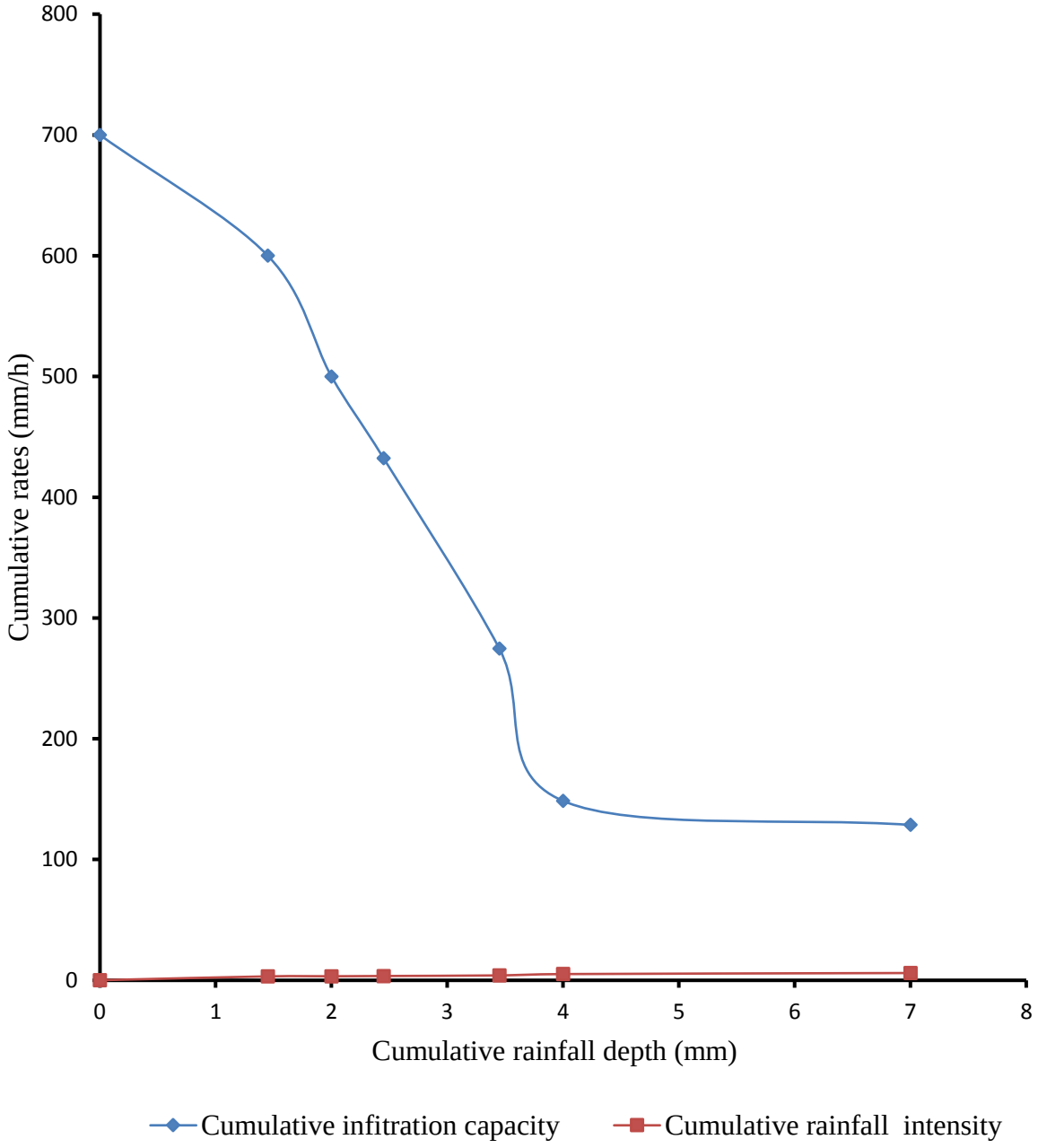


**Figure 4. 8:** Ponding in natural forest

From Figure 4.9, for the natural forests in higher rainfall intensities are required for ponding to be realized. The infiltration rate in natural forest was high such that no ponding occurred for the 82 minutes rainfall storm. The soil structural stability consequently led to increase in macro pores and consistency in pore space on the sub surface soil hence reduction in surface runoff. Figure 4.10 represented the behaviour of the 82 minutes storm in the grassland.

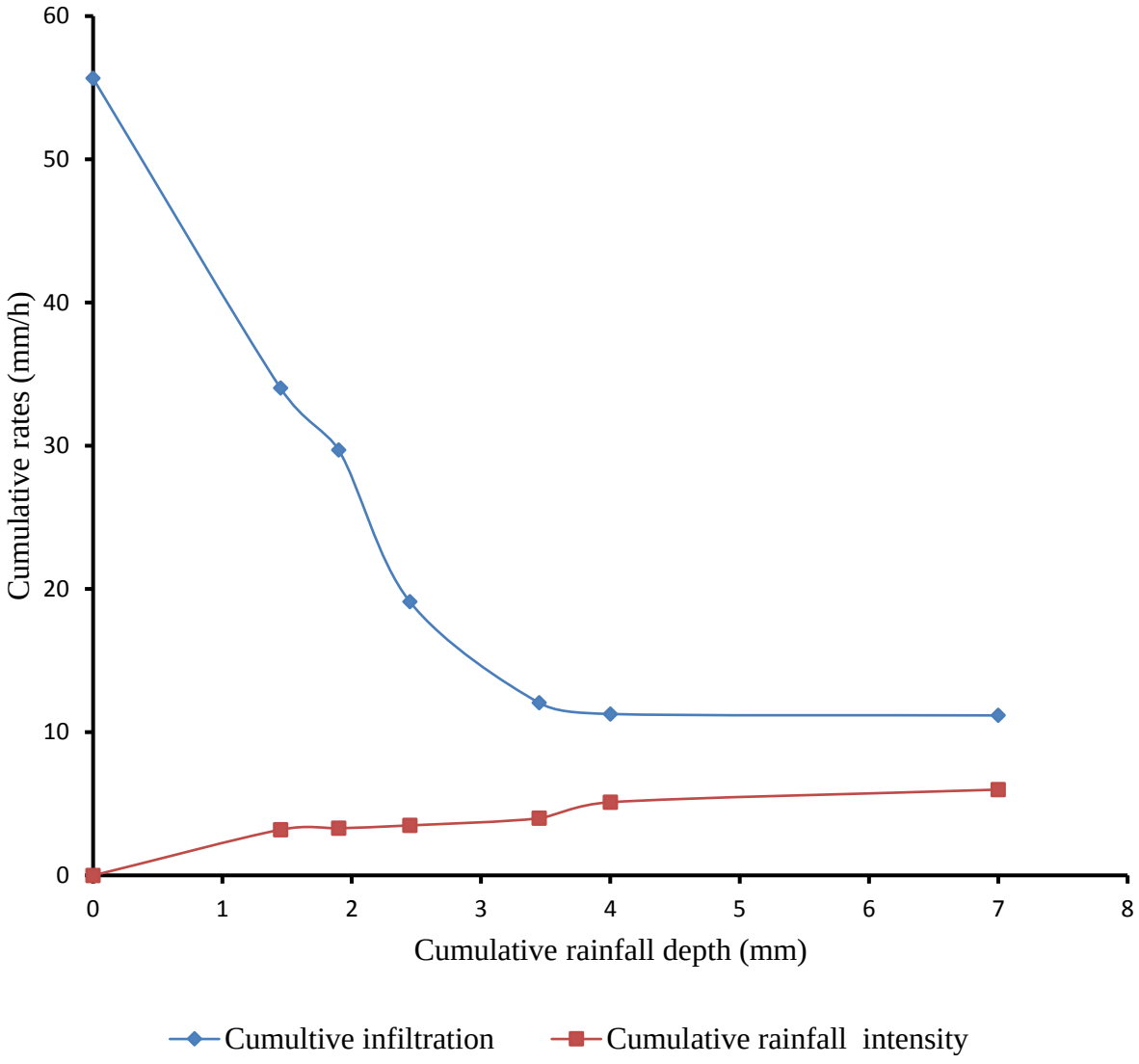


**Figure 4.9:** Ponding in grassland

The response of soil in the grassland was not significantly different from the fallow agricultural land and natural forest as shown in the Figure 4.10. During the 82 minutes rainfall with varying intensities ponding could not be achieved. This was due to high infiltration rates that were experienced in the grassland. Figure 4.11 shows the storm in the deforested land and ponding time determination.

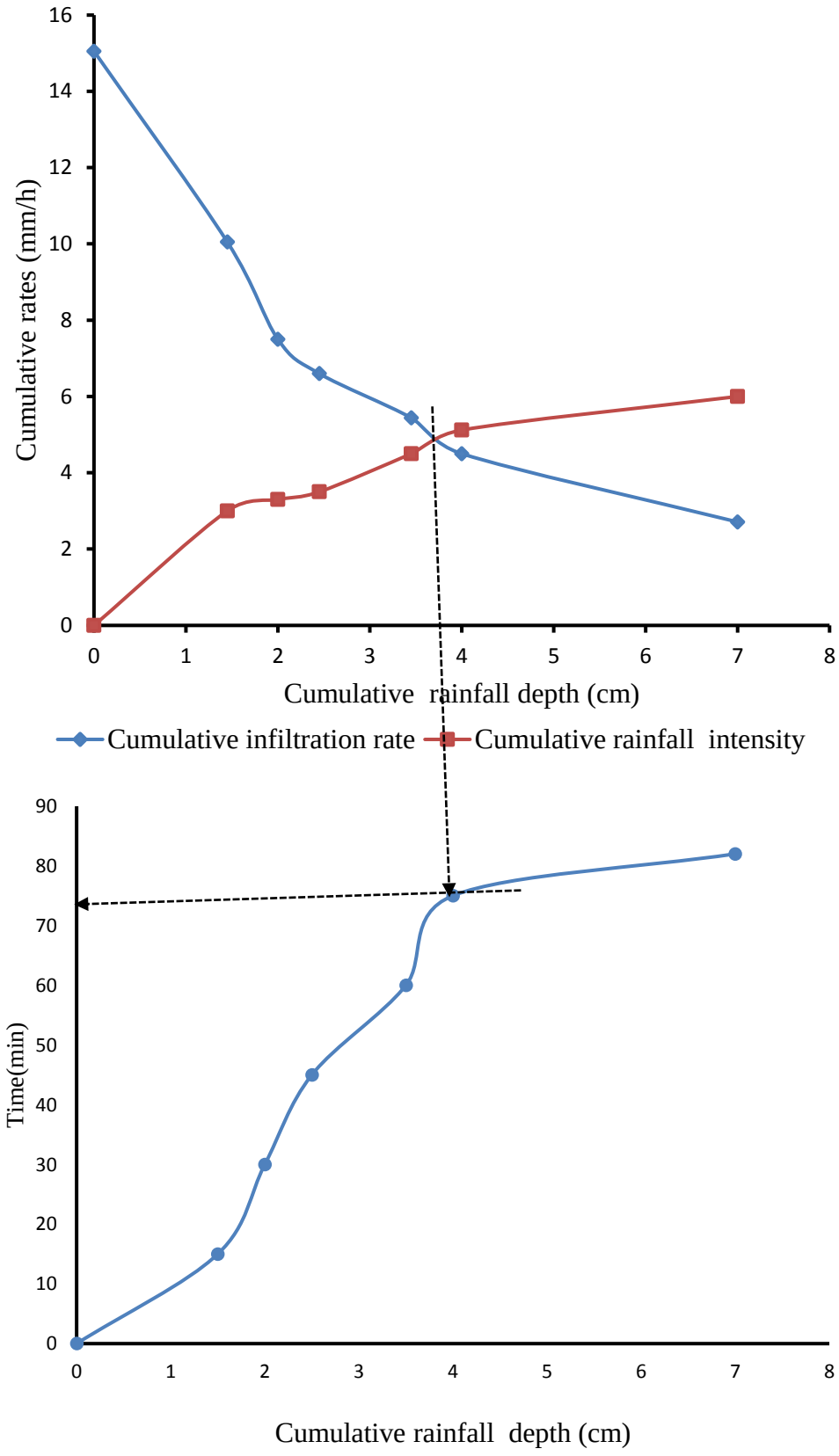


**Figure 4. 10:** Ponding time determination

The soil hydrologic response in the deforested land was different as compared to the other land use types as shown in Figure 4.11. The time of ponding is at the point where the intersection of the graphs coincide. Ponding time was achieved at 70 minute for a storm of duration 82 minutes. The quick response in ponding could be due to low vegetation cover and deterioration of the soil structure due to compaction hence reducing infiltration rate of soil in the area. This concur with Zwartendijk *et al.* (2017) findings that infiltration rates in mature forests was characterized by macro pores flow delayed ponding while deforested land is characterized by matrix -flow hence faster ponding.

### 4.1.8 Correlation between Soils Hydrologic Response Parameters

Correlation tests were carried out between saturated hydraulic conductivity and other soil hydrologic parameters. The infiltration capacity and porosity were found to have a positive relationship with saturated hydraulic conductivity in the different land use types with coefficients of 0.42 and 0.998 respectively. On the other hand, runoff coefficient, bulk density and soil water content had a negative correlation with saturated hydraulic conductivity (-0.92 and -0.998). The results showed that land use change had caused a negative impact on the soil hydrological properties hence changing soil functioning in ways that reduced rainfall infiltration due to reduction of soil saturated hydraulic conductivity.

## 4.2 Event-based Rainfall Partitioning

### 4.2.1 Gross Rainfall

Table 4.2 presented the frequency distribution of the gross rainfall (GR) depth that was collected during the study period of October to December 2017. The GR depths were classified into three classes depending on the depth of the rainfall as shown.

**Table 4. 2:** The frequency distribution of events depending on depth

| GR class (mm) | Frequency | GR (mm) |
|---|---|---|
| < 10 | 18 (64.3%) | 53.7 (21.7%) |
| 10-20 | 7 (25%) | 99.6 (40.3%) |
| >20 | 3 (10.7%) | 93.8 (38%) |

There were twenty-eight events that were recorded and grouping the rainfall events depending on the depth, the extreme event had a depth of 41.8 mm while the least had a depth of 0.5 mm hence a range of 41.3 mm. Rainfall events having a depth of less than 10 mm were often

experienced. There were 18 events having rainfall depth of less than 10 mm which represented 64.3 % of the total events. In the second category of events of depth 10-20 mm there were 7 events which were 25 % of the total events. There were events having rainfall depth of more than 20 mm hence 10.7 % of the total number of events. The events having a depth of less than 10mm resulted into a cumulative depth of 53.7 mm hence 21.7 % of the total gross rainfall depth. The cumulative GR depths for events between 10-20 mm and greater than 20 mm were 99.6 and 93.8 mm with 40.3 % and 38 % respectively of the total GR. The mean gross rainfall depth (GR) was 8.83 mm while the cumulative depth was 247.1 mm. The gross rainfall depth for the month of October was 134.2 mm while for the month of November was 112.9 mm.

### 4.2.2 Through Flow, Stem Flow and Interception

The partitioning of the gross rainfall into through flow (TF), stem flow (SF) and interception loss is presented in the Table 4.3. The net rainfall (NR) was equal to the sum of stem flow and through flow.

**Table 4. 3:** Cumulative, mean and standard deviation of rainfall partitions

| | GR<br>mm | TF&SF<br>mm | I<br>mm |
|---|---|---|---|
| Cumulative | 247.10 | 106.36 | 148.80 |
| Mean | 8.83 | 3.80 | 5.03 |
| Standard deviation | 9.90 | 4.43 | 6.54 |

During the study, cumulative through flow (*TF*) and stem flow depths (*SF*) was 106.36 mm which represented 43.04 % of the gross rainfall while the mean TF and SF was 3.8 mm as shown in Table 4.3. The cumulative interception loss depth was 148.80 mm representing 56.96 % of the GR and the mean depth was 5.028 mm. The cumulative NR depth was 106.36 mm while the mean depth was found to be 3.8 mm which was 43.04% of the GR. The sum of TF and SF was found to be equal to NR. This indicated that the rainfall reaching the ground surface was as a result of through flow and stem flow. The standard deviation for the GR, SF, TF and I were 9.899, 4.43, 6.54 and 4.43 respectively. The findings were consistent with Winkler *et al*. (2010) who argued that regeneration of tree stand lowly increases the rainfall interception losses at the site. Nonetheless effect of forest regeneration on hydrological processes is affected by several factors that include; weather, biophysical characteristics of the catchment and forest

disturbance. The associated factors could also contribute to high interception losses as compared to net rainfall. The deviations between interception and stem and through flow could be due to the method used. As reviewed by Crockford & Richardson (2000), characteristics of the forest that affect interception that include: branch angle, the uniformity of crown, leaf shape, index and inclination are very difficult to identify and quantify hence could lead to more interception losses during computation.

### 4.2.3 Through Flow, Stem Flow and Gross Rainfall

The relationship between the TF, SF and GR was as shown in Figure 4.12.

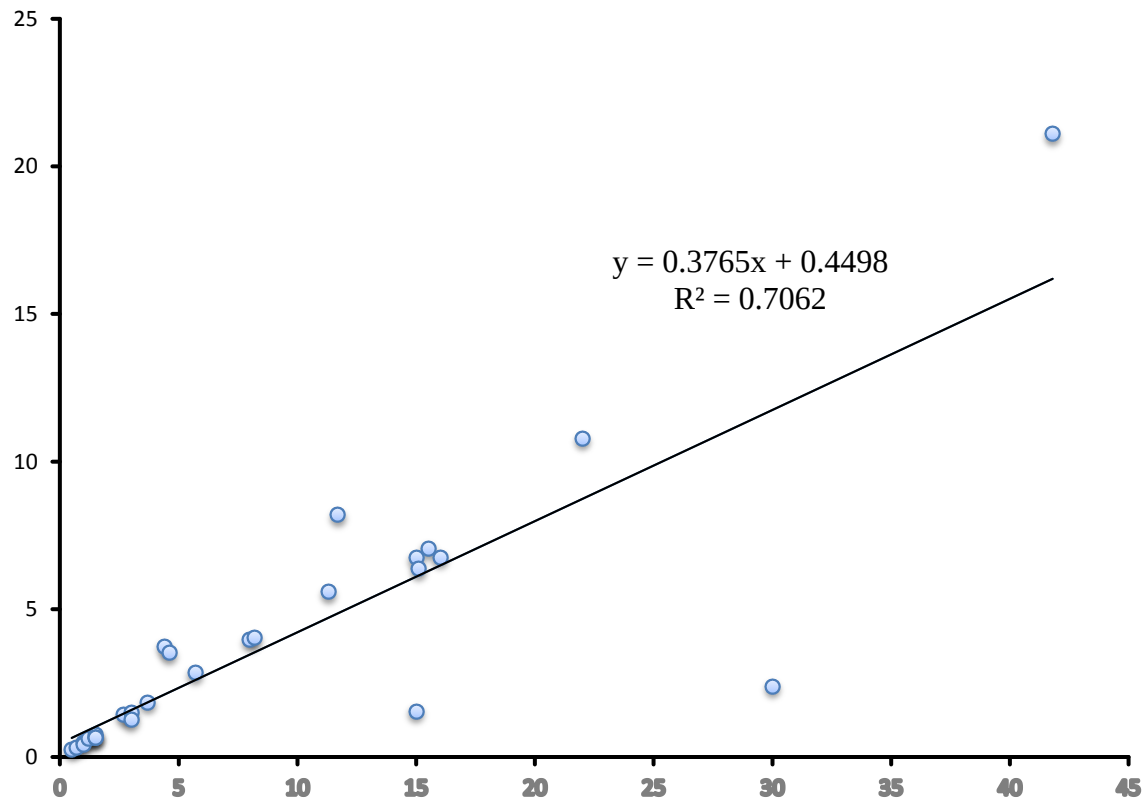


**Figure 4. 11:** Through and stem flow and gross rainfall

Based on Figure 4.12, there was a strong positive linear correlation observed between TF, SF and GR with $R^2 = 0.706$. This relationship reveals that there was high production of TF and SF during high rainfall events while during low rainfall events the TF and SF production reduced. Rainfall events of less than 5 mm depth resulted to very low amounts of TF and SF thus more water was intercepted. The findings are in line with Ahmadi *et al.* (2009) who carried out a study on the partitioning rainfall into through fall, stem flow, and interception loss in an oriental

beech forest during the growing season and found a positive linear relationship between the TF, SF and GR. The results were also consistent with the findings of Bahmani *et al.* (2012) who carried out a study in the Caspian Forest of Iranthe and found a strong positive correlation of between TF, SF and GR with $R^2$ = 0.98 and 0.74 respectively.

The amount of TF and SF was found to be equal to the amount of NR since it was the amount of water reaching the ground surface. Therefore reduction in TF and SF leads to reduction in NR reaching the ground surface. A study conducted by Munishi & Shear (2005) on rainfall interception and partitioning in afro-montane forest of the eastern mountains in Tanzania for the implication of water conservation showed that through fall and stem flow showed similar increasing trends with increasing amount of monthly precipitation. The findings further indicated that regression of the monthly through flow and stem flow against gross precipitation indicated a linear relationship. A single ANOVA analysis was carried out between the GR and TF and SF at $p$ = 0.05. The results ($p$ = 0.018) indicated that there was significant difference between gross rainfall and through fall and stem flow that was generated.

### 4.2.4 Interception Loss and Gross Rainfall

Analysis of the relationship between the interception losses is key since it influences the water balance. Figure 4.13 presented the findings obtained

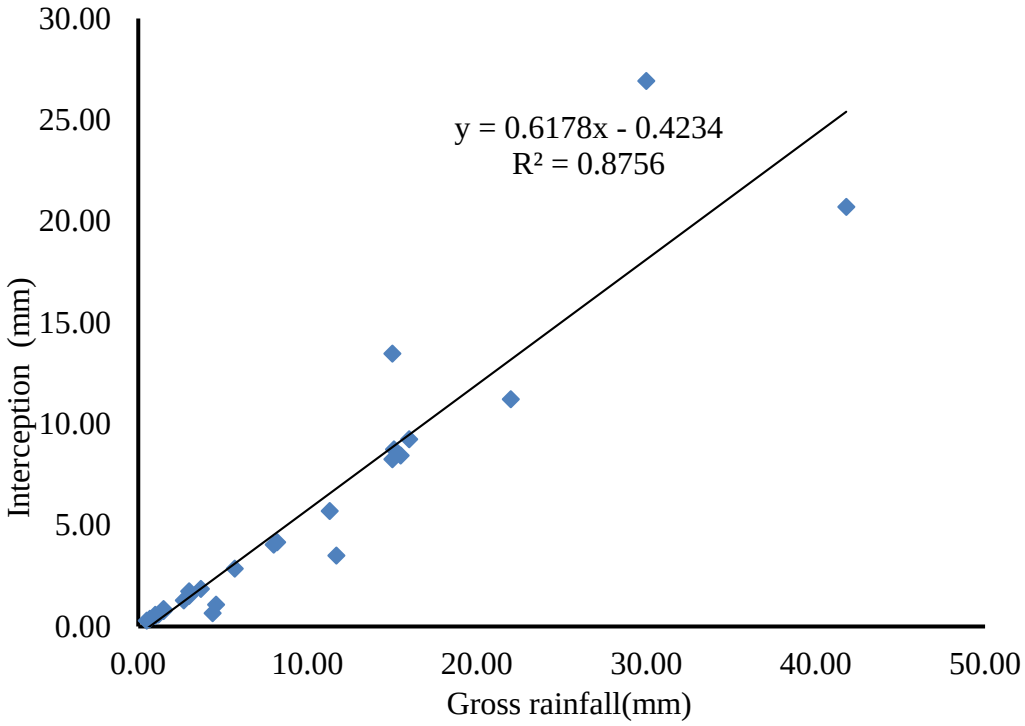


**Figure 4.12:** Interception loss and gross rainfall

From the results, there was a positive power regression ($R^2$ =0.8756) between I and GR. The findings showed that the proportion of GR that was intercepted by red stink wood canopy declined as the magnitude of the rainfall events increased. This could be due to less impact of rainfall events of low magnitude on the canopy hence most of the rain water being intercepted. The findings are in line with Yi-Ying & Ming-Hsu (2016) who carried out a study on the quantifying rainfall interception loss of subtropical broadleaved forest in central Taiwan. Their findings showed that a simple linear regression relationship ($R^2 = 0.75$). The study was carried out during the period when the trees were green hence high amounts of interception experienced. However the findings of Staelens *et al.* (2008) showed that during the leafless period, the magnitudes of the interception were negative. The high interception loss could be due to high percentage of leaf area since it was during the rainy season.

### 4.3 Comparison of Probability Distribution functions

The probability distribution functions were compared in terms of peak discharge estimation and their results are given in the subsequent sections.

#### 4.3.1 Variations in Peak Discharges

The variations in the annual peak discharges for Njoro River at the gauging station 2FC05 were as shown in Figure 4.14.

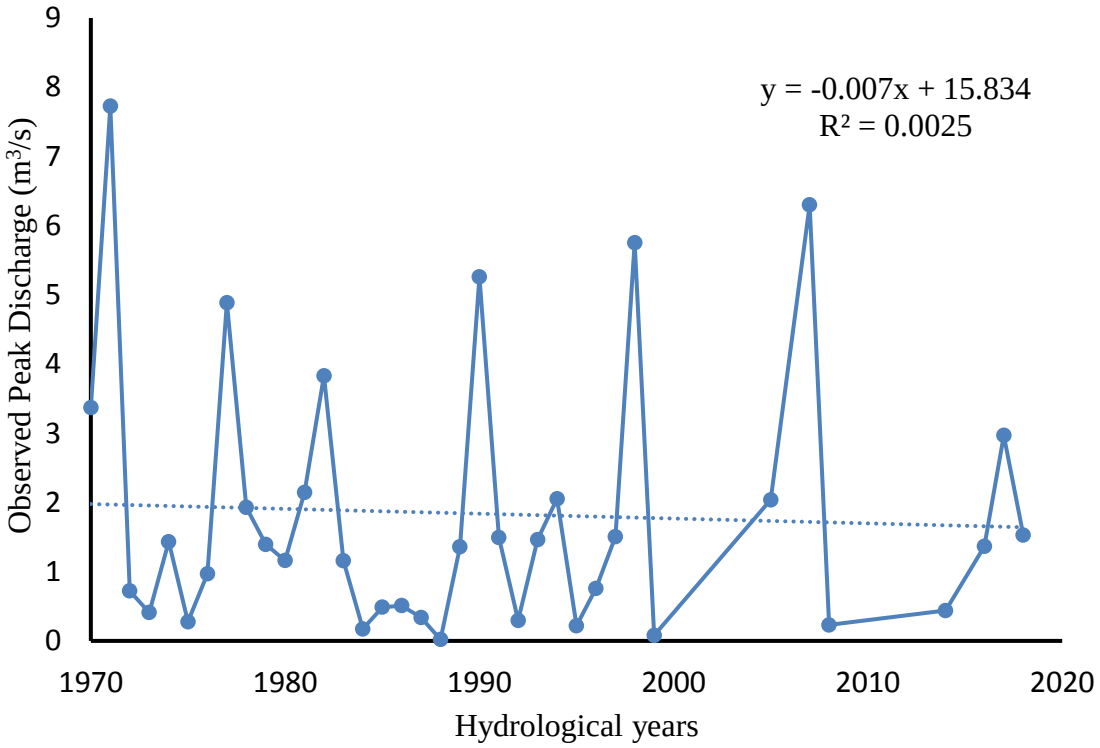


**Figure 4. 13:** Variation in peak discharge at 2FC05

The highest and lowest flows were 7.70 and 0.08 $m^3/s$ in the years 1971 and 1999 respectively. The average flow for the study period was 1.84 $m^3/s$. There were five major peak discharges exceed 4.9 $m^3/s$ observed in 1971, 1977, 1990, 1998 and 2007. The fluctuations in the discharges were associated to deforestation since Mwetu (2010) observed reduction in forest cover of 22 % in the period of 1973-2000.

### 4.3.2 Probability Distribution and Goodness of Fit Tests

The best fitting probability distribution model was Generalized Pareto followed by Weibull (3P), Log-Pearson 3 and Generalized Extreme Value respectively. The best parameters estimated for were as shown in Table 4.4.

**Table 4. 4:** Best fit parameters

| Probability function | Parameters |
|---|---|
| Generalized Pareto | $k=0.14967$ , $\sigma=1.5267$ , $\mu=-0.0216$ |
| Weibull (3P) | $\alpha=0.85374$ , $\beta=1.535$ , $\gamma=0.0213$ |
| Log-Pearson 3 | $\alpha=6.1258$ , $\beta=0.53429$ , $\gamma=3.2111$ |
| Generalized Extreme Value | $k=0.3385$ , $\sigma=0.91817$ , $\mu=0.79738$ |

Based on Table 4.4 for Generalized Pareto distribution parameters, k represents shape, σ is the standard deviation and μ is the mean. The findings are in line with Romali & Yusop (2017) who carried out frequency analysis annual flood in Segamat River in Malaysia and found Generalized Pareto to be the best fitting probability distribution model within the catchment. The probability density function (pdf**)** for the best fit probability models are shown in Figure 4.15 which shows frequency of different observations.

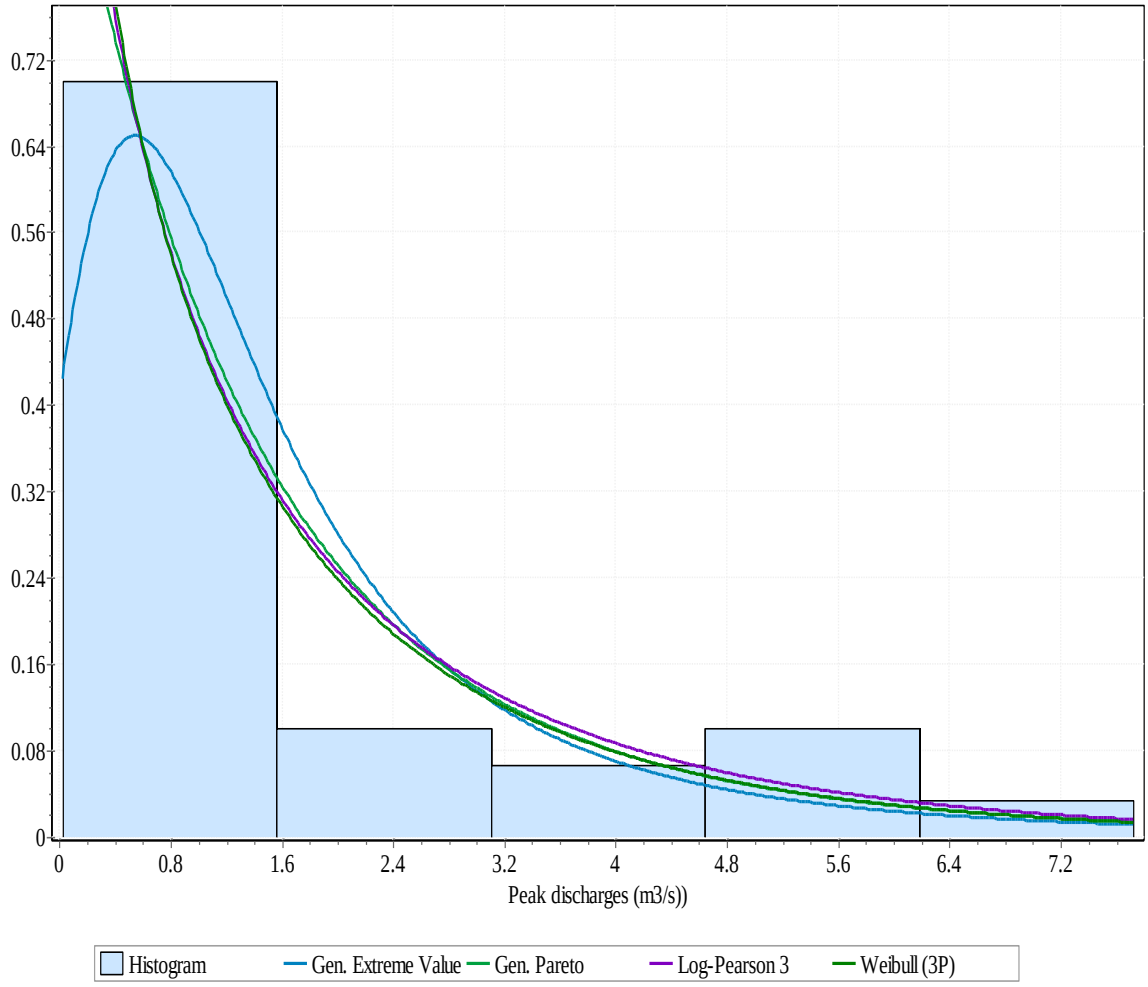


**Figure 4. 14:** Histogram and probability density functions

The histogram of maximum annual peak discharge showed a bimodal distribution. The probability density functions revealed Generalized Pareto, Log-Pearson 3 and Weibull (3P) to have similar probability densities with corresponding higher frequencies as compared to Generalized Extreme Value distributions. Figure 4.16 shows the cumulative density functions of the four best fitting probability distribution models values equal or less than the observations.

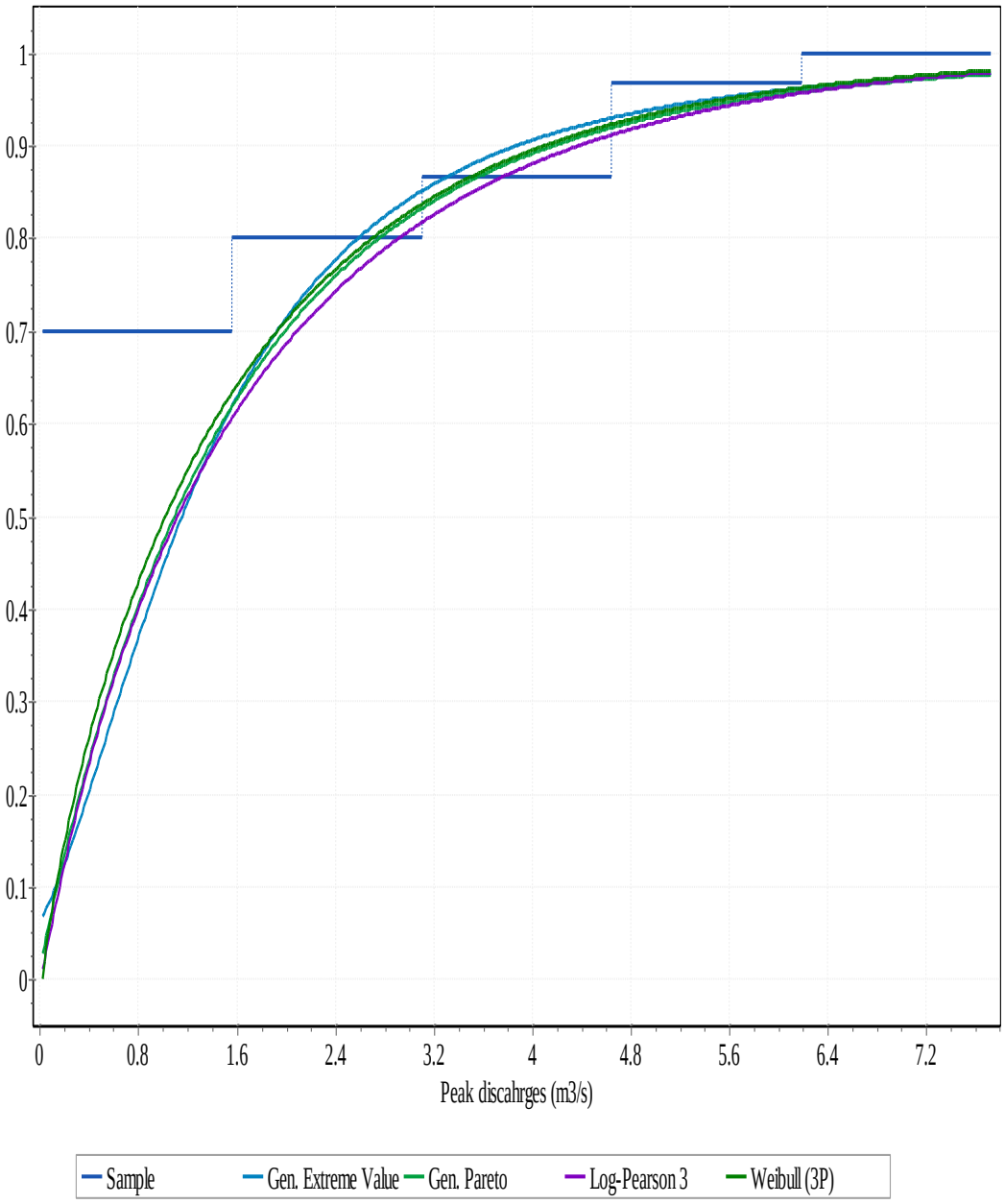


**Figure 4. 15:** Cumulative density functions

The results from Figure 4.16, showed non-exceedence probability for a given magnitude. There was an indication that the cumulative peak discharge were increasing with increase in probability. In addition, at higher probabilities of up to 1, the magnitude of peak discharges could not be exceeded. Figure 4.17 showed the probability-probability plot which represented the cumulative density function (cdf) empirical values against theoretical cdf values.

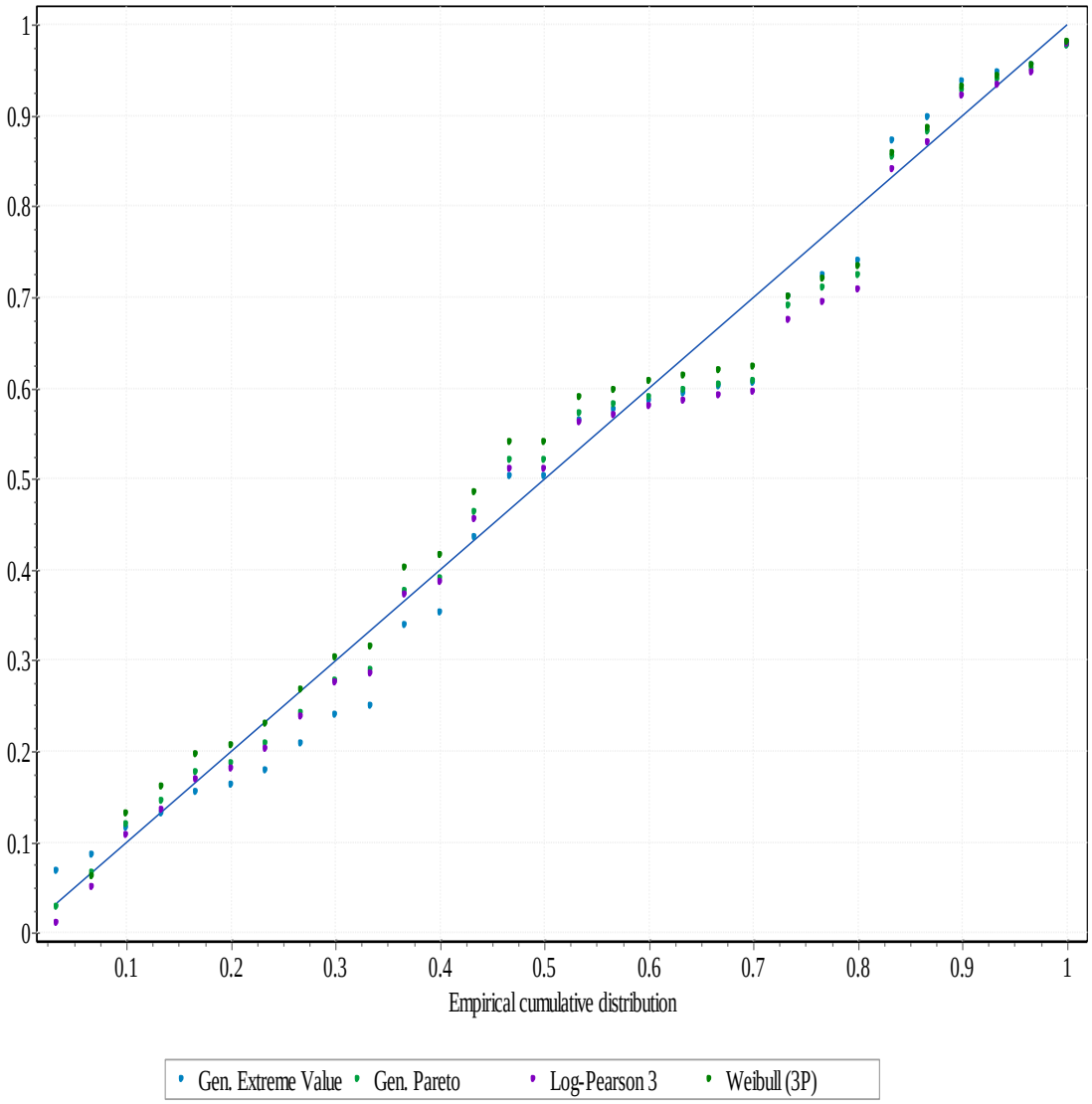


**Figure 4. 16:** Probability-Probability plot

The Probability –Probability plot indicated how well a specific distribution fitted the observed data. The distribution that had most values close to the line was Generalized Pareto and hence the best fit probability distribution model. The findings were in line with Romali & Yusop (2017) who carried out frequency analysis annual flood in Segamat River in Malaysia and found Generalized Pareto to be the best fitting probability distribution model within the catchment. Figure 4.18 showed the distribution of probability difference which represented the difference between empirical cumulative density function values and theoretical cumulative density function values.

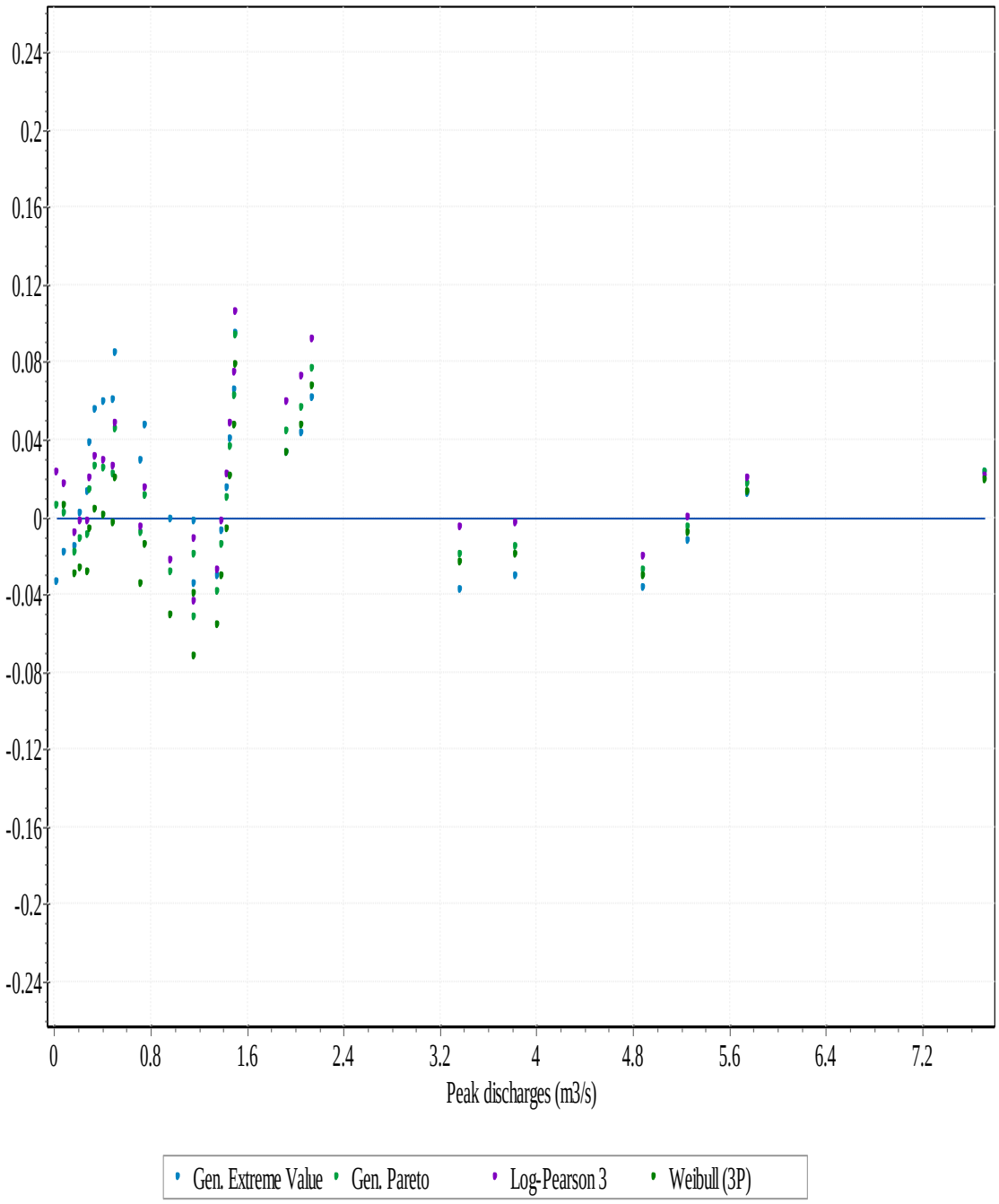


**Figure 4. 17:** Probability difference

There was an indication that Generalized Pareto distribution model fitted well for the observed peak discharges in Njoro River at Egerton gauge station (1D. 2FC05). There was also an indication of increase frequency for higher discharges within the catchment and decrease in frequency for lower discharges which could be attributed to deforestation. The finding concur

with Ahmad *et al*. (2015) who found Generalized Pareto to be the most suitable model for analysis of annual maximum streamflow in Pakistan.

### 4.3.3 Estimation of Peak Discharge for different return periods

Peak flow discharges corresponding to the return periods of 2, 5, 10, 100 and 200 years were estimated using the Generalized Pareto which was the best fitting probability model. The estimated discharges were as shown in Figure 4.19

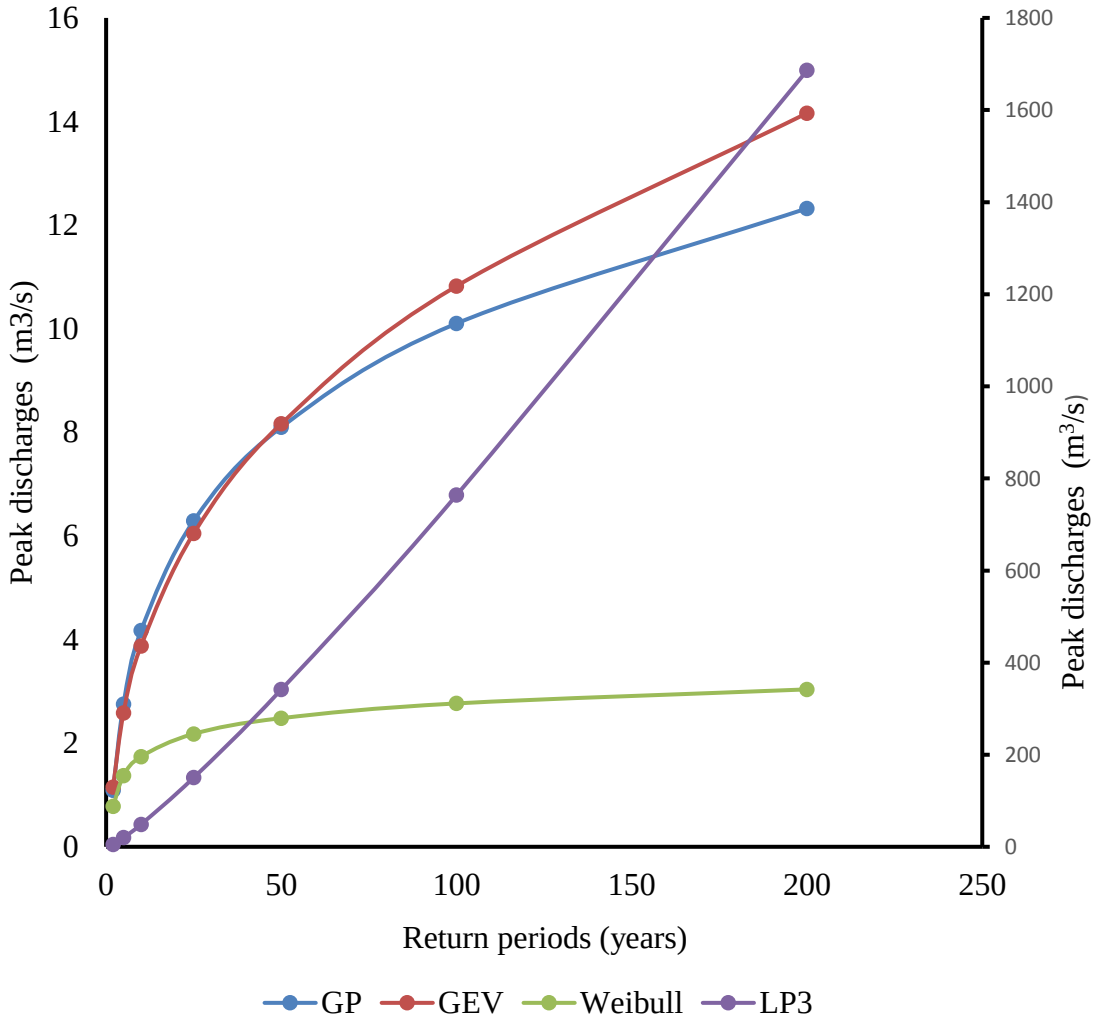


**Figure 4. 18:** Estimated discharges for different return periods

The four models showed increasing discharges at higher return periods as shown in Figure 4.19. The estimated flows were close to the observed. The increasing flows could be associated to deforestation being experienced within the catchment. This also agrees with Karanja *et al*. (1985) who carried out a study in the catchment and found that intensive cultivation on fragmented land appeared to lower flow rate of the river. The findings concur with Kundu *et*

*al*. (2014) who carried out a study in Livuvhu River Catchment and found out that the frequency of floods of high magnitudes were increasing although the increase was attributed it to climate change. A study by Mwetu (2010) revealed that the hydrological behaviour of River Njoro was threatened by forest excision and encroachment as compared to climate variability. Simulation results by Baker & Miller (2013) indicated that land use changes had resulted in corresponding increases in surface runoff and decreases in groundwater recharge hence affecting the hydrologic behaviour especially in the uppermost reaches of the catchment.

# CHAPTER FIVE
# CONCLUSIONS AND RECOMMENDATIONS

## 5.1 Conclusions

The findings showed that the highest and lowest mean bulk density of 1.36 and 0.96 g/cm$^3$ was recorded for deforested and natural forest land respectively. The highest mean saturated hydraulic conductivity (170.21 cm/day), porosity (0.62) and organic matter content (4.63 %) were observed in the natural forest while the lowest values (24.78 cm/day, 0.47 and 0.75 %) respectively were found in the deforested land. There were implications that soil properties that influenced soil hydrologic response were significantly affected in the deforested areas hence affecting hydrological functioning in the UNRiC. The results also indicated that there were significant differences in soil hydrological response parameter among different land use types land uses types in UNRiC. It was also observed that deforestation had led to changes in soil properties that influence hydrologic response and generation of stream flow. The findings also showed that soil hydrological behavior was influenced by land use to a large extent. In addition, there was evident that deforestation and logging had led to soil compaction due to high bulk density recorded hence reducing continuity in the macro-pore flow therefore negatively impacting soil hydrological functioning.

Based on results of rainfall partitioning, the value of the mean net rainfall (NR) was 56.96 % of the gross rainfall (GR) while through flow and stem flow were 43.04 % of the GR. The fraction of interception loss which is equal to net rainfall determines the hydrological behaviour of a forest. The findings of the study indicated that partitioning of gross rainfall into net rainfall and interception loss was influenced to a large extent by the magnitude of the rainfall event. The tested species of the tree showed to have a good dumping effect to storms hence reduction in the impact of raindrops on the soil which will reduce erosion within the catchment

Best fitting probability distribution for peak annual discharge of Njoro River gauging station 2FC05 was determined by testing different probability distribution models. The best fitting model was found to be Generalized Pareto followed by Weibull, Log-Pearson 3 and Generalized Extreme Value probability distribution model. Peak flow discharges estimated for the return periods of 50, 100 and 200 using the best fitting model included 8.1, 10.1 and 12.3 m$^3$/s respectively. The frequency analysis of the peak flows showed increasing discharges at higher probabilities of exceedence at all return periods. This information is key for flood risk

mapping and planning. The study has provided knowledge on hydrologic responses to rainfall events essential for developing policies that address soil water resources conservation and evaluation of risks linked to changing land use practices.

### 5.2 Recommendations

The following recommendations were made;

i. Determination of soil properties and soil hydrologic response parameters during wet, dry and transition period to provide a better understanding of soil hydrologic response within the Upper Njoro River Catchment.

ii. A comparative study of rainfall partitioning for different stages of forest growth that include mature forests, semi-mature and regenerating forest for decision support in the soil hydrological functioning restoration within the catchment.

iii. Use of different goodness of fit ranking techniques to compare with the results for this study and analysis of low flow trends to be able to set minimum flows recommended to protect stream values.

## REFERENCES


Abegaz, A., & Adugna, A. (2015). Effects of soil depth on the dynamics of selected soil properties among the highlands resources of Northeast Wollega, Ethiopia: are these sign of degradation? *Solid Earth Discussions*, 7(3), 2011-2035.

Abu-Hashim, M. S. D. (2011). Impact of land-use and land-management on the water infiltration capacity of soils on a catchment scale. JKI.

Ahmadi, M. T., Attarod, P., Mohadjer, M. R. M., Rahmani, R., & Fathi, J. (2009). Partitioning rainfall into throughfall, stemflow, and interception loss in an oriental beech (Fagus orientalis Lipsky) forest during the growing season. *Turkish Journal of Agriculture and Forestry*, 33(6), 557-568.

Afreen, S., & Muhammad, F. (2012). Flood frequency analysis of various dams and barrages in Pakistan. *Irrigation and drainage*, 61(1), 116-128.

Ahmad, I., Fawad, M., & Mahmood, I. (2015). At-Site Flood Frequency Analysis of Annual Maximum Stream Flows in Pakistan Using Robust Estimation Methods. *Polish Journal of Environmental Studies*, *24*(6), 2345-2353.

Alam, M. A., Emura, K., Farnham, C., & Yuan, J. (2018). Best-Fit Probability Distributions and Return Periods for Maximum Monthly Rainfall in Bangladesh. *Climate, 6(1), 9-25.*

Alletto, L., & Coquet, Y. (2009). Temporal and spatial variability of soil bulk density and near-saturated hydraulic conductivity under two contrasted tillage management systems. *Geoderma*, 152(1-2), 85-94.

Amer, A. M., Suarez, C., Valverde, F., Carranza, R., Matute, L., & Delfini, G. (2014). Saturated Hydraulic Conductivity Changes with Time and Its Prediction at SAR and Salinity in Quevedo Region Soils. *Journal of Water Resource and Protection*, 6(17), 1561-1573.

Amin, M. T., Rizwan, M., & Alazba, A. A. (2016). A best-fit probability distribution for the estimation of rainfall in northern regions of Pakistan. *Open Life Sciences*, *11*(1), 432-440.

Arcenegui, V., Mataix-Solera, J., Guerrero, C., Zornoza, R., Mayoral, A. M., & Morales, J. (2007). Factors controlling the water repellency induced by fire in calcareous Mediterranean forest soils. *European Journal of Soil Science,* 58(6), 1254-1259.

Assefa , K, & Moges ,M. A. (2018). Low flow trends and frequency analysis in Blue Nile Basin, Ethiopia. *Journal of water resources and protection,* 10, 182-203.

Assouline, S. (2004). Rainfall-induced soil surface sealing. *Vadose Zone Journal*, 3(2), 570-591.

Assouline, S., & Mualem, Y. (2000). Modeling the dynamics of soil seal formation: Analysis of the effect of soil and rainfall properties. *Water Resources Research*, 36(8), 2341-2349.

Assouline, S., Selker, J. S., & Parlange, J. Y. (2007). A simple accurate method to predict time of ponding under variable intensity rainfall. *Water resources research*, 43(3), 1-10.

Bahmani, S. M. H. G., Attarod, P., Bayramzadeh, V., Ahmadi, M. T., & Radmehr, A. (2012). Throughfall, stemflow, and rainfall interception in a natural pure forest of chestnut-leaved oak (Quercus castaneifolia CA Mey.) in the Caspian Forest of Iran. *Annals of Forest Research*, 55(2), 197-206.

Baker, T. J., & Miller, S. N. (2013). Using the Soil and Water Assessment Tool (SWAT) to assess land use impact on water resources in an East African watershed. *Journal of Hydrology,* 486, 100-111.

Beckett, P. H. T. (1971). Soil variability: a review. *Soils and fertilizers*, *34*(1), 1-15.

Benavides, I. F., Solarte, M. E., Pabón, V., Ordoñez, A., Beltrán, E., Rosero, S., & Torres, C. (2018). The variation of infiltration rates and physical-chemical soil properties across a land cover and land use gradient in a Paramo of southwestern Colombia. *Journal of Soil and Water Conservation*, 73(4), 400-410.

Beven, K. (2004). Robert E. Horton's perceptual model of infiltration processes. *Hydrological processes,* 18(17), 3447-3460.

Bhagat, N. (2017). Flood Frequency Analysis Using Gumbel's Distribution Method: A Case Study of Lower Mahi Basin, India. *Journal of Water Resources and Ocean Science,* 6(4), 51-54.

Bobee, B. B., & Robitaille, R. (1977). The use of the Pearson type 3 and log Pearson type 3 distributions revisited. *Water Resources Research*, 13(2), 427-443.

Bouyoucos, G. J. (1962). Hydrometer method improved for making particle size analyses of soils 1. *Agronomy journal*, 54(5), 464-465.

Bruijnzeel, L. A. (2004). Hydrological functions of tropical forests: not seeing the soil for the trees? *Agriculture, ecosystems & environment*, 104(1), 185-228.

Brutsaert, W. (2005). *Hydrology: an introduction*. Cambridge University Press.

Buttle, J. M., Beall, F. D., Webster, K. L., Hazlett, P. W., Creed, I. F., Semkin, R. G., & Jeffries, D. S. (2018). Hydrologic response to and recovery from differing silvicultural systems in a deciduous forest landscape with seasonal snow cover. *Journal of Hydrology*, 557, 805-825.

Cerda, A., Schnabel, S., Ceballos, A., & Gomez-Amelia, D. (1998). Soil hydrological response under simulated rainfall in the Dehesa land system (Extremadura, SW Spain) under drought conditions. Earth Surface Processes and Landforms*: The Journal of the British Geomorphological Group*, 23(3), 195-209.

Chandramouli, S., & Natarajan, N. (2016). A Comparative Study on the Infiltration Characteristics of Soils in Srikakulam District, Andhra Pradesh, India. *Asian Journal of Water, Environment and Pollution*, 13(1), 73-79.

Charlier, J. B., Moussa, R., Cattan, P., Cabidoche, Y. M., & Voltz, M. (2009). Modelling runoff at the plot scale taking into account rainfall partitioning by vegetation: application to stemflow of banana (Musa spp.) plant. *Hydrology and Earth System Sciences Discussions*, 13, 2151-2168.

Chow, V.,M Maidment, D. R., & Mays, L. W. (1998). *Applied hydrogeology*. In: McGraw-Hill Book Co, New York.

Clemmens, A. (1983). Infiltration equations for border irrigation models.

Correa, A., Windhorst, D., Crespo, P., Célleri, R., Feyen, J., & Breuer, L. (2016). Continuous versus event-based sampling: how many samples are required for deriving general hydrological understanding on Ecuador's páramo region?. *Hydrological Processes, 30(22)*, 4059-4073.

Crockford, R. H., & Richardson, D. P. (2000). Partitioning of rainfall into throughfall, stemflow and interception: effect of forest type, ground cover and climate. *Hydrological processes*, *14*(16-17), 2903-2920.

Croke, B. F. W., Merritt, W. S., & Jakeman, A. J. (2004). A dynamic model for predicting hydrologic response to land cover changes in gauged and ungauged catchments. *Journal of Hydrology*, 291(1-2), 115-131.

Doerr, S. H., Shakesby, R. A., Dekker, L. W., & Ritsema, C. J. (2006). Occurrence, prediction and hydrological effects of water repellency amongst major soil and land-use types in a humid temperate climate. *European Journal of Soil Science*, 57(5), 741-754.

dos Santos, K. F., Barbosa, F. T., Bertol, I., de Souza Werner, R., Wolschick, N. H., & Mota, J. M. (2018). Study of soil physical properties and water infiltration rates in different types of land use. *Semina: Ciências Agrárias*, *39*(1), 87-98.

Dos Santos, V., Laurent, F., Abe, C., & Messner, F. (2018). Hydrologic Response to Land Use Change in a Large Basin in Eastern Amazon. *Water*, 10(4), 429-449.

Engda, T. A., Bayabil, H. K., Legesse, E. S., Ayana, E. K., Tilahun, S. A., Collick, A. S., & Steenhuis, T. S. (2011). Watershed hydrology of the (semi) humid Ethiopian Highlands. In Nile River Basin 145-162.

Fisher, R. F., & Binkley, D. (2000). Forest soils. New York, NY: J.

Friday, I. A. and Runyi, E. F. (2018). Comparison of goodness of fit test for normal distribution. *Asian Journal of Probability and Statistics* ,1 (2) ,1-32.

Göl, C., & Yilmaz, H. (2017). The effect of land use type/land cover and aspect on soil properties at the gökdere catchment in northwestern turkey. *Šumarski list*, *141*(9-10), 459-467.

Guzha, A. C., Rufino, M. C., Okoth, S., Jacobs, S. and Nóbrega, R. L. B. (2018). Impacts of land use and land cover change on surface runoff, discharge and low flows: Evidence from East Africa. *Journal of Hydrology: Regional Studies, 15, 49-67.*

Haghighi, F., Gorji, M., & Shorafa, M. (2010). A study of the effects of land use changes on soil physical properties and organic matter. *Land Degradation & Development*, *21*(5), 496-502.

Havel, A., Tasdighi, A., & Arabi, M. (2018). Assessing the hydrologic response to wildfires in mountainous regions. *Hydrology and Earth System Sciences*, *22*(4), 2527.

Philip, J. R. (1954). An infiltration equation with physical significance. *Soil Science*, *77*(2), 153- 158.

Hillel, D. (1998). Environmental soil physics: Fundamentals, applications, and environmental considerations. Elsevier.

Hilten, R. N., Lawrence, T. M., & Tollner, E. W. (2008). Modeling stormwater runoff from green roofs with HYDRUS-1D. *Journal of Hydrology*, *358*(3-4), 288-293.

Horton, R. E. (1942). Simplified method of determining an infiltration-capacity curve from an infiltrometer-experiment. *Eos, Transactions American Geophysical Union,* 23(2), 570-575.

Ice, G. G., Neary, D. G., & Adams, P. W. (2004). Effects of wildfire on soils and watershed processes. *Journal of Forestry*, *102*(6), 16-20.

Karanja, A. K., China, S. S., & Kundu, P. (1986). The influence of land use on Njoro River catchment between 1975 and 1985. Soil and Water Conservation in Kenya.

Karanth, K. (1987). Ground water assessment: development and management: Tata McGraw-Hill Education

Kostiakov, A. N. (1932). On the dynamics of the coefficient of water-percolation in soils and on the necessity of studying it from a dynamic point of view for purposes of amelioration. *Trans. 6th Cong. International. Soil Science, Russian Part A*, 17-21.

Kroes, J. G., Van Dam, J. C., Groenendijk, P., Hendriks, R. F. A., & Jacobs, C. M. J. (2009). *SWAP version 3.2. Theory description and user manual* (No. 1649 (02)). Alterra.

Kundu, P. M., China, S. S., Chemelil, M. C., & Onyando, J. O. (2004, July). Detecting and quantifying land cover and land use change in Eastern Mau by Remote Sensing. In *20th ISPRS Congress. Istanbul, Turkey*. 37, 1-5.

Kundu, P. M., Singo, L. R., Odiyo, J. O., & Mathivha, F. I. Impact of Land Cover change on Stream Discharges and Water Resources in Luvuvhu River Catchment

Kutílek, M., & Nielsen, D. R. (1994). Soil hydrology: Textbook for students of soil science, agriculture, forestry, geoecology, hydrology, geomorphology and other related disciplines. Catena Verlag.

Lemenih, M. (2004). *Effects of land use changes on soil quality and native flora degradation and restoration in the highlands of Ethiopia*, 306, 1-70.

Lewis, M. (1937). The rate of infiltration of water in irrigation-practice. *Eos, Transactions American Geophysical Union*, *18*(2), 361-368.

Lin, H., & Zhou, X. (2008). Evidence of subsurface preferential flow using soil hydrologic monitoring in the Shale Hills catchment. *European Journal of Soil Science*, *59*(1), 34-49.

Lu, Z., Zou, S., Qin, Z., Yang, Y., Xiao, H., Wei, Y., & Xie, J. (2015). Hydrologic responses to land use change in the loess plateau: case study in the upper fenhe river watershed. *Advances in Meteorology*, *2015*.

Mainuri, Z. G., & Owino, J. O. (2013). Effects of land use and management on aggregate stability and hydraulic conductivity of soils within River Njoro Watershed in Kenya. *International Soil and Water Conservation Research*, *1*(2), 80-87.

Mataix-Solera, J., Arcenegui, V., Guerrero, C., Mayoral, A. M., Morales, J., González, J. & Gómez, I. (2007). Water repellency under different plant species in a calcareous forest soil in a semiarid Mediterranean environment. *Hydrological Processes: An International Journal*, *21*(17), 2300-2309.

Merriam, E. R., Fernandez, R., Petty, J. T., & Zegre, N. (2017). Can brook trout survive climate change in large rivers? If it rains. *Science of the Total Environment*, *607*, 1225-1236.

Mishra, S. K., & Singh, V. P. (2013). Soil conservation service curve number (SCS-CN) methodology (Water Science and Technology), Springer amazon digital library, 42, 1-83.

Mockus, V. (1964). National Engineering Handbook.

Moges, A., Dagnachew, M., & Yimer, F. (2013). Land use effects on soil quality indicators: a case study of Abo-Wonsho Southern Ethiopia. *Applied and Environmental Soil Science*, 2013, 1-10.

Moreno-de las Heras, M., Nicolau, J. M., Merino-Martín, L., & Wilcox, B. P. (2010). Plot-scale effects on runoff and erosion along a slope degradation gradient. *Water Resources Research*, *46*(4), 1-12.

Munishi, P. K. T., & Shear, T. H. (2005). Rainfall interception and partitioning in afromontane rain forests of the Eastern Arc Mountains, Tanzania: Implications for water conservation. *Journal of tropical forest science*, 17 (3), 355-365.

Mwetu, K. K. (2010) . Modelling Responses of Hydrology to Land Use/ Land Cover Change and Climate Variability: A case of River Njoro Catchment of Kenya:Doctoral Thesis .University of Natural Rsources and Applied Sciences , Vienna.

Negassa, W. (2001). Assessment of important physicochemical properties of Dystric Udalf (Dystric Nitosols) under different management systems in Bako area, western Ethiopia. A thesis presented to School of graduate studies, Alemaya University, Ethiopia.

Niazi, M., Nietch, C., Maghrebi, M., Jackson, N., Bennett, B. R., Tryby, M., & Massoudieh, A. (2017). Storm water management model: performance review and gap analysis. *Journal of Sustainable Water in the Built Environment*, *3*(2), 1-33.

Okelo, M. O., Onyando, J. O., Shivoga, W. A., & Miller, S. N. (2015). Assessment of infiltration using a mini rainfall simulator in the river njoro watershed. In Proceedings of Taal 2007: The 12th World Lake Conference. 777, 786- 796.

Onda, Y., Dietrich, W. E., & Booker, F. (2008). Evolution of overland flow after a severe forest fire, Point Reyes, California. *Catena*, *72*(1), 13-20.

Ouko, C. M., Maryanne, O. A., & Mark, B. K. (2016). Assessment of hydrological impacts of Mau Forest, Kenya. *Hydrology: Current Research*, *7*(1).

Owens, M. K., Lyons, R. K., & Alejandro, C. L. (2006). Rainfall partitioning within semiarid juniper communities: effects of event size and canopy cover. *Hydrological Processes: An International Journal*, 20(15), 3179-3189.

Patil, V. S., Chavan, S. M. and Pawar, D. P. (2018). Spatial distribution of soil under the influence of infiltration rate. *Journal of Pharmacognosy and Phytochemistry*, 7(2), 2024-2029.

Philip, J. (1957). The theory of infiltration: 1. The infiltration equation and its solution. *Soil Science*, 83(5), 345-358.

Raude, J. M. (2006). Determination of surface runoff and soil loss under varying rainfall intensity in selected land use practices in River Njoro catchment of Kenya: Msc. Thesis: Egerton University, Kenya.

Rawls, W. J. (1993). Infiltration and soil water movement. *Handbook of hydrology*.

Romali, N. S., & Yusop, Z. (2017). Frequency Analysis of Annual Maximum Flood for Segamat River. In *MATEC Web of Conferences*. 103-1012.

Santra, P., Kumar, M., Kumawat, R. N., Painuli, D. K., Hati, K. M., Heuvelink, G. B. M., & Batjes, N. H. (2018). Pedotransfer functions to estimate soil water content at field capacity and permanent wilting point in hot Arid Western India. *Journal of Earth System Science, 127*(3), 35.

Schneiderman, E. M., Steenhuis, T. S., Thongs, D. J., Easton, Z. M., Zion, M. S., Neal, A. L. & Todd Walter, M. (2007). Incorporating variable source area hydrology into a curve-number-based watershed model. *Hydrological Processes: An International Journal*, *21*(25), 3420-3430.

Schwen, A., Bodner, G., Scholl, P., Buchan, G. D., & Loiskandl, W. (2011). Temporal dynamics of soil hydraulic properties and the water-conducting porosity under different tillage. *Soil and Tillage Research*, *113*(2), 89-98.

Sharma, T. C., & Panu, U. S. (2015). Predicting return periods of hydrological droughts using the Pearson 3 distribution: a case from rivers in the Canadian prairies. *Hydrological Sciences Journal, 60(10), 1783-1796.*

She, N., & Pang, J. (2009). Physically based green roof model. *Journal of Hydrologic Engineering*, *15*(6), 458-464.

Skaggs, R. W., & Khaleel, R. (1982). Infiltration. *Hydrologic modeling of small watersheds. ASAE Monogr*, *5*, 121-166.

Soil Survey Division Staff (1993) Soil Survey Manual. Soil Conservation Service. *US* Department of Agriculture Handbook, 18, 315.

Staelens, J., De Schrijver, A., Verheyen, K., & Verhoest, N. E. (2008). Rainfall partitioning into throughfall, stemflow, and interception within a single beech (Fagus sylvatica L.) canopy: influence of foliation, rain event characteristics, and meteorology. *Hydrological Processes: An International Journal*, *22*(1), 33-45.

Surhartanto E., Limantara , L.M., Noviadriana D., Harta , F. I. and Aryani , K.D. (2018) .Estimation of design flood with four frequency analysis distributions .*Asian Journal of applied science and Technology 2 (1), 13-27*

Tilahun, C., & Asefa, T. (2009). Assessment of soil organic matter under four land use systems in Bale highlands, Southeast Ethiopia: A. Soil organic matter contents in four land use systems: forestland, grassland, fallow land and cultivated land. *World Applied Sciences Journal*, *6*(9), 1231-1246.

Tilahun, S. A., Guzman, C. D., Zegeye, A. D., Engda, T. A., Collick, A. S., Rimmer, A., & Steenhuis, T. S. (2013). An efficient semi-distributed hillslope erosion model for the subhumid Ethiopian Highlands. *Hydrology and Earth System Sciences*, *17*(3), 1051-1063.

Tuffour, H. O., Asare, J. and Nutakor, G. M. (2018). Prediction of infiltration from soil hydraulic properties. *Eurasian Journal of Soil Science, 7(1), 64-72.*

Utin, U. E., & Oguike, P. C. (2018). Available online www. jsaer. Com. *Journal of Scientific and Engineering Research*, *5*(6), 79-87.

Van't Woudt, B. D. (1969). Resistance to wetting under tropical and subtropical conditions. In *Water Repellent Soils. Proceedings of the Symposium on Water Repellent Soils. Univ. Calif., Riverside*

Winkler, R. D., Moore, R. D., Redding, T. E., Spittle house, D. L., Smerdon, B. D., & Carlyle-Moses, D. E. (2010). The Effects of Forest Disturbance on Hydrologic Processes and Watershed. Compendium of forest hydrology and geomorphology in British Columbia. BC.

Yimer, F., Messing, I., Ledin, S., & Abdelkadir, A. (2008). Effects of different land use types on infiltration capacity in a catchment in the highlands of Ethiopia. *Soil use and management*, *24*(4), 344-349.

Zwartendijk, B. W., van Meerveld, H. J., Ghimire, C. P., Bruijnzeel, L. A., Ravelona, M., & Jones, J. P. G. (2017). Rebuilding soil hydrological functioning after Sweden agriculture in eastern Madagascar. *Agriculture, ecosystems & environment*, *239*, 101-111.

# APPENDICES

## Appendix A: Figures

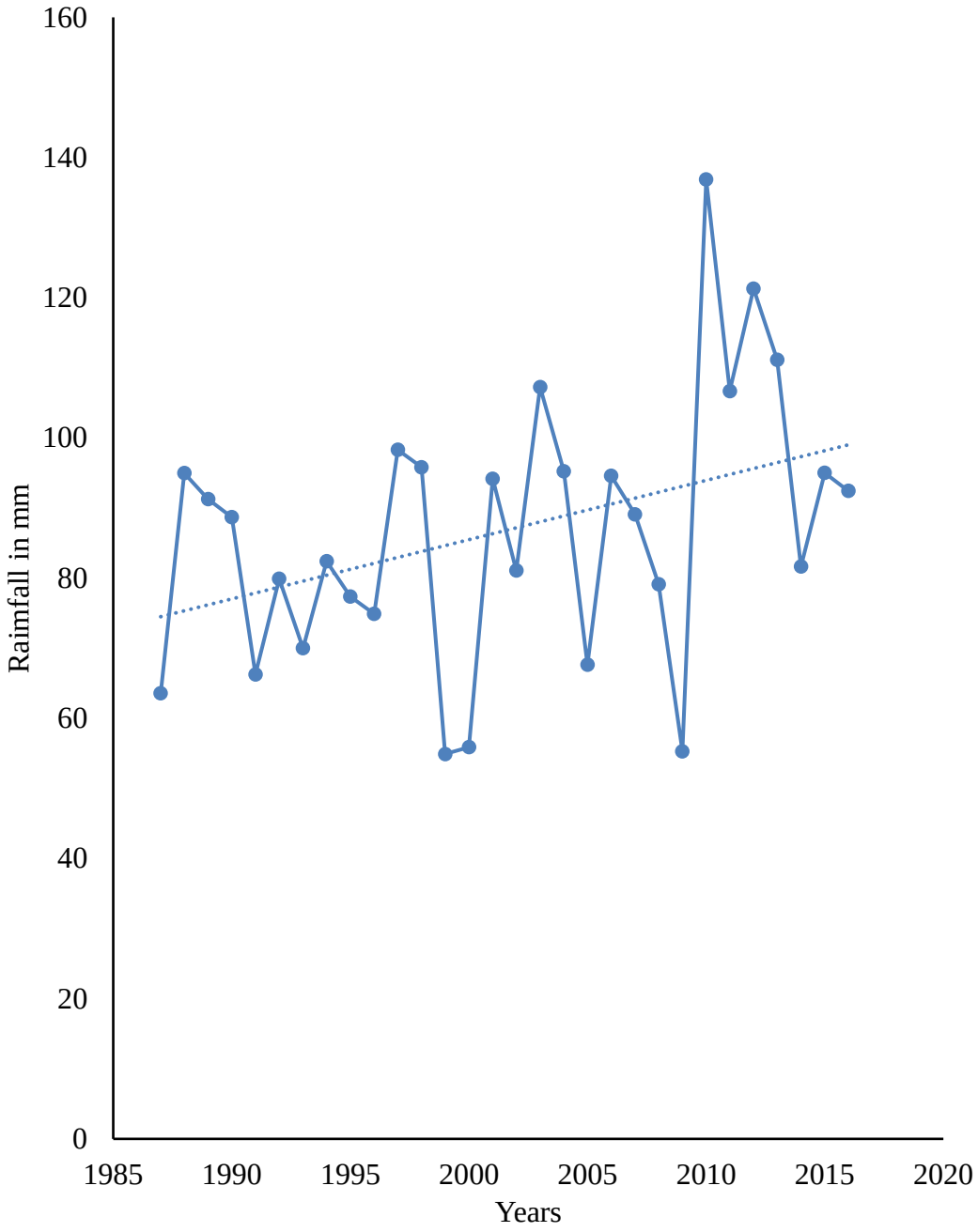


**Appendix A. 1 :** Average monthly rainfall patterns for Upper Njoro River Catchment.

## Appendix B: Plates


**Appendix B. 1** : Soil texture determination

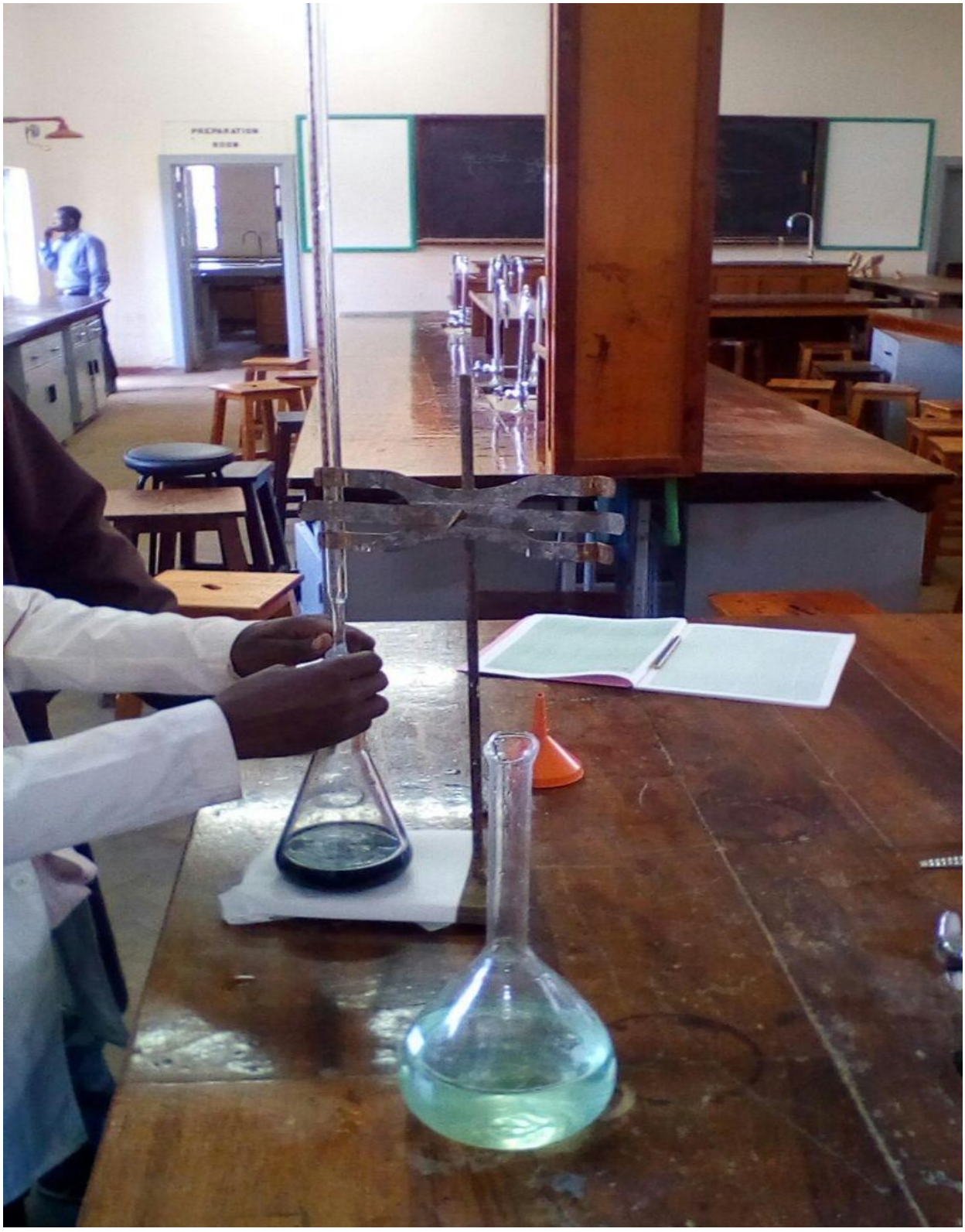

**Appendix B. 2**: Soil organic carbon determination

**Appendix B. 3:** Double ring infiltration Test Setting up

**Appendix B. 4 :** Infiltration test set-up

**Appendix B. 5**: Rainfall partitioning set-up

**Appendix C:** Tables

**Appendix C. 1 :** Soil properties in different land use types

| Land use | BD | Porosity | $K_{sat}$ | Field capacity |
|---|---|---|---|---|
| Agricultural | 1.26 | 0.53 | 83.80 | 4.5 |
| Grassland | 1.01 | 0.61 | 169.93 | 3.9 |
| Deforested | 1.36 | 0.47 | 12.78 | 3.7 |
| Natural forest | 0.97 | 0.62 | 170.21 | 5.6 |

**Appendix C. 2:** Analysis of variance for infiltration

| Source of Variation | SS | df | MS | F | P-value | F crit |
|---|---|---|---|---|---|---|
| Between Groups | 53940.65 | 3 | 17980.22 | 8.681213 | 0.000445 | 3.008787 |
| Within Groups | 49707.94 | 24 | 2071.164 | | | |
| Total | 103648.6 | 27 | | | | |

**Appendix C. 3:** Temporal variations in bulk density and Ksat

| | Location | | Month | | | | | | |
|---|---|---|---|---|---|---|---|---|---|
| Land use | East | North | Sep | | Oct | | Nov | | Dec | |
| | | | BD | Ksat | BD | Ksat | BD | Ksat | BD | Ksat |
| Natural forest | 35.93 | -0.36 | 0.87 | 138.60 | 1.00 | 146.7 | 1.02 | 110.59 | 0.98 | 170.2 |
| Agric land | 35.95 | -0.37 | 1.17 | 54.40 | 1.23 | 83.80 | 1.32 | 54.4 | 1.30 | 86.20 |
| Grassland | 35.92 | -0.35 | 0.90 | 160.30 | 1.03 | 159.0 | 1.06 | 151.7 | 1.03 | 169.3 |
| Deforested | 35.92 | -0.37 | 1.30 | 22.20 | 1.41 | 18.29 | 1.40 | 12.78 | 1.34 | 23.2 |

**Appendix C.4:** Analysis of ANOVA for rainfall partitioning

| Source of Variation | SS | df | MS | F | P-value | F crit |
|---|---|---|---|---|---|---|
| Between Groups | 360.4792 | 1 | 360.4792 | 5.986871 | 0.017829 | 4.026631 |
| Within Groups | 3131.005 | 52 | 60.21163 | | | |
| Total | 3491.484 | 53 | | | | |

**Appendix C.5:** Water repellency class for the tested points on the catchment

| Land use | Eastings | Northings | $P_t$ | Class |
|---|---|---|---|---|
| Natural forest | 35.93 | -0.36 | 5 | Very low |
| Fallow agric land | 35.95 | -0.37 | 8 | Very low |
| Grassland | 35.92 | -0.35 | 15 | Low |
| Deforested | 35.92 | -0.37 | 18 | Low |

**Appendix C.6:** Estimated Peak discharges ($cm^3/s$)

| Return Period (Years) | Exceedence Probability (%) | Non-Exceedence Probability (%) | Estimated Discharges ($m^3/s$) GP | GEV | LP3 | Weibull |
|---|---|---|---|---|---|---|
| 2 | 50 | 50 | 1.0935 | 1.154 | 5.3567 | 0.783 |
| 5 | 20 | 80 | 2.7568 | 2.585 | 19.97 | 1.373 |
| 10 | 10 | 90 | 4.1756 | 3.8769 | 48.9 | 1.742 |
| 25 | 4 | 96 | 6.2919 | 6.0478 | 150.3 | 2.180 |
| 50 | 2 | 98 | 8.0971 | 8.1655 | 341.7 | 2.483 |
| 100 | 1 | 99 | 10.1 | 10.822 | 763.8 | 2.768 |
| 200 | 0.5 | 99.5 | 12.321 | 14.161 | 1686.0 | 3.039 |